THE UNIVERSITY OF MICHIGAN
COLLEGE OF ENGINEERING
Department of Engineering Mechanics

Special Technical Report

PLANE STRESS SOLUTIONS BASED ON THE COULOMB YIELD CRITERION

M. D. Coon
R. M. Haythornthwaite

ORA Project 05894

under contract with:

DEPARTMENT OF THE ARMY
ORDNANCE TANK-AUTOMOTIVE COMMAND
DETROIT ORDNANCE DISTRICT
CONTRACT NO. DA-20-018-AMC-0980T
DETROIT, MICHIGAN

administered through:

OFFICE OF RESEARCH ADMINISTRATION ANN ARBOR

April 1965

This report is based on a dissertation submitted by M.D. Coon in partial fulfillment of the requirements for the degree of Doctor of Philosophy in The University of Michigan, 1965.

TABLE OF CONTENTS

	Page
LIST OF TABLES	iv
LIST OF FIGURES	v
ABSTRACT	vii
CHAPTER	
I. INTRODUCTION	1
II. LIMIT ANALYSIS OF BEAMS AND PLATES IN CYLINDRICAL BENDING	8
A. Yield Surface	8
B. Solutions	14
III. LIMIT ANALYSIS OF A CYLINDRICAL SHELL	18
A. Generalized Stresses and Strain Rates	21
B. Yield Criterion and Flow Rule	23
C. Analysis of a Cylindrical Shell Loaded with a Ring of Pressure	36
D. Numerical Results	46
IV. PLASTIC ANALYSIS OF AN ANNULAR PLATE	56
A. Basic Equations	57
B. Solutions	60
1. Type 1 Solution	61
2. Type 2 Solution	67
V. CONCLUSIONS	71
A. Limit Analysis of Beams and Plates in Cylindrical Bending	72
B. Limit Analysis of a Cylindrical Shell	72
C. Plastic Analysis of an Annular Plate	73
REFERENCES	75

LIST OF FIGURES

FIGURE		Page
2-1.	Beam loaded by moment M and axial force F.	10
2-2.	Stress-strain diagram.	10
2-3.	Fully plastic stress distribution in a beam.	10
2-4.	Yield curve for a rectangular beam for $N^2 = 1$ and $N^2 = 4$.	13
2-5.	A beam restrained from rotation at the ends and loaded by a concentrated load P at the center.	14
2-6.	The ratio of the limit loads of a fully restrained beam to a beam restrained from rotation as a function of N^2.	17
3-1.	Plane stress section of Coulomb yield criterion.	20
3-2.	Cylindrical shell element.	21
3-3.	Strain rate distribution in shell element.	26
3-4.	Strain rate distribution in shell element.	29
3-5.	Section of the yield surface for a cylindrical shell with $n_x = 0$ for $N^2 = 1$ and $N^2 = 4$.	33
3-6.	Section of the yield surface for a cylindrical shell with $m_x = 0$ for $N^2 = 1$ and $N^2 = 4$.	34
3-7.	Section of the yield surface for a cylindrical shell with $n_\theta = 0$ for $N^2 = 1$ and $N^2 = 4$.	35
3-8.	Cylindrical shell loaded by a ring of pressure.	36
3-9.	Limit load as a function of N^2.	47
3-10.	Longitudinal moment as a function of distance.	49
3-11.	Circumferential normal stress resultant as a function of distance.	50

LIST OF FIGURES (Concluded)

FIGURE		Page
3-12.	Longitudinal shear stress resultant or radial velocity as a function of distance.	51
3-13.	A typical distribution of the stress resultant for internal loading.	54
4-1.	Plane stress section of Coulomb yield criterion.	58
4-2.	Annular plate. a) Undeformed plate, b) Type I deformation of the plate, c) Type II deformation of the plate.	58
4-3.	Limit load of annular plate as a function of plate size.	69

ABSTRACT

Methods of plastic analysis of structures which were originally developed for materials in which yield is unaffected by mean stress are extended to materials which exhibit a dependence. Well known experimental evidence suggests that this more general material model would be appropriate for some soil and rock structures, and may be of use for such diverse materials as concrete, ice, and plastics.

The analysis is concerned with the ideal rigid/plastic model of the mathematical theory of plasticity. The complete mathematical description of a rigid/plastic material must include a yield criterion which specifies the states of stress for which flow is possible and a flow rule which relates these states of stress to the velocities which are associated with them. For this description the Coulomb yield criterion, which is linearly dependent on mean stress, is chosen because of its mathematical simplicity and because of a record of successful application to plane strain problems of soil mechanics. The flow rule which is associated with the Coulomb yield criterion by the ideal rigid/plastic theory predicts dilatation of the material in the deforming region of a structure. This feature is absent in previous analyses based on materials in which yield is insensitive to mean stress and where, as a consequence, deformation occurs at constant volume.

Attention is confined to structures such as beams, plates, and shells where the stress state can adequately be described as plane. A basic shell element is considered in detail and the nature of the yield surface expressed in terms of generalized forces is delineated. The analyses used here are generalizations of those used for materials which are independent of mean stress. These generalizations are needed to account for the dilatation of the deforming material.

The yield surface developed for the shell element is employed in the limit analysis of a long cylindrical shell loaded by a ring of pressure. Two different cases of loading are compared: one in which the ring of pressure is applied from the inside and the other with the ring of pressure applied from the outside. A natural consequence of the dependence of the Coulomb yield criterion on mean stress is that the limit load for the externally applied load is greater than that for the internally applied load.

The limit load analysis of ideal plasticity predicts only the loads at zero deformation and the associated initial velocites. For

many structures this information is sufficient; however, there are cases in which information concerning continuing motion is desirable. For example, the expansion pressures of an annular plate by in-plane pressure can be adequately described only by considering finite displacements. This problem illustrates the modifications which must be made in the plastic analysis when using the Coulomb yield criterion and its associated flow rule for finite displacements. The limit load of an annular plate is found for all ratios of the outside radius to the inside radius. In addition, the stress distribution, velocity, displacement, thickening, and extent of the deformable region are found for finite displacements limited only by the range of validity of the assumption concerning plane stress conditions.

CHAPTER I

INTRODUCTION

In the theory of continuum mechanics, there are two types of relations: (1) basic principles which are valid for all materials (e.g. conservation of mass, conservation of energy, balance of momentum, etc.), and (2) constitutive equations which describe the particular material being considered. The constitutive equations which describe a rigid/plastic material are the yield criterion which determines under what states of stress motion is possible and a flow rule which relates these states of stress to the strain rates. Therefore, when attempting to solve boundary value problems in plasticity, a yield criterion and flow rule must be chosen which adequately describe the most important aspects of the particular material being studied.

Most of the boundary value problems which have been solved using the theory of plasticity have utilized the Tresca or Mises yield criteria or an approximation to one of these. These criteria are used because they can represent adequately the yielding of metals and their alloys in most of which yield is unaffected by a superimposed hydrostatic pressure (e.g. see R. Hill [1]). However, when the theory of plasticity is applied to soil mechanics problems, the Coulomb yield criterion is used because it approximates the available experimental data [2-4] very closely. The most significant difference between the

Coulomb yield criterion and the Tresca or Mises yield criteria is that the Coulomb yield criterion is linearly dependent on mean stress whereas the yield criteria of Tresca and Mises are independent of mean stress. There are materials such as cast iron, concrete, some plastics, ice, and compacted snow which cannot be adequately described by using any yield criterion which is independent of mean stress. At present, there is not enough experimental evidence to completely describe the yield criteria associated with these materials. But the fact that these materials exhibit different tensile and compressive yield stresses [5-10] is sufficient to determine that they cannot be described by either the Tresca or Mises yield criteria without anisotropic effects. The Coulomb yield criterion does predict different tensile and compressive yield stresses and therefore might be used to describe these materials. Also, from the standpoint of solving boundary value problems involving these materials the Coulomb yield criterion seems to be a logical choice because of its mathematical simplicity and because it has been used successfully in soil mechanics problems. Materials such as cast iron, concrete, plastics, ice, and compacted snow can be used as structural materials. Therefore, it is of some interest to determine to what extent problems involving beams, plates, shells, etc. can be analyzed using the Coulomb yield criterion.

With the hope of obtaining most of the important features of structural problems, the solutions obtained in this work will involve a material which is rigid/perfectly plastic and which obeys the Coulomb

yield criterion. Of course, to obtain plasticity solutions, to all but statically determinate problems, a flow rule must be used together with the yield criterion. For the work done here, the ideally plastic flow rule associated with the Coulomb yield criterion will be used. For the ideally plastic flow rule, the plastic potential from which the strain increment vectors are derived is identical with the yield criterion. Graphically this can be interpreted as requiring that the strain increment vector is normal to the yield surface on any regular regime* and on a singular regime,** the strain increment vector can be any linear combination with positive coefficients of the strain increment vector of the adjacent regimes. The use of the ideally plastic flow rule is desirable because it is the only one for which the uniqueness of the limit load has been established. Also, methods for determining upper and lower bounds on the limit load have been developed when this flow rule is used (e.g. see W. Prager [11]).

The use of the Coulomb yield criterion together with its associated flow rule does present difficulties which are not present when using either the Tresca or Mises yield criteria. First, the Coulomb yield surface can change both size and shape as the material properties change, whereas the Tresca and Mises surfaces can only change size. This leads to solutions which are two parameter families of the material properties in contrast to the one parameter families obtained from the

*Regime with a continuously turning tangent.
**Regime with no unique normal.

Tresca and Mises criteria. Secondly, the flow rule associated with the Coulomb yield criterion predicts dilatation, whereas the flow rules associated with the Tresca and Mises criteria predict incompressibility of the material. The problem of dilatation is made more difficult because there are different expressions for the dilatation associated with different regimes of the yield surface.

The difficulties in obtaining solutions to plasticity problems are in many ways common to all problems of non-linear continuum mechanics. However, there are two questions peculiar to plasticity that must be answered tentatively before a problem can be started, namely, "Which facets of the yield surface will be involved?" and "What is the size and shape of the deformable region?" The first question can sometimes be circumvented by using the upper and lower bound theorems of plasticity in conjunction with an approximate yield surface. The approximate surface may have fewer facets and therefore the problem of deciding which facets are involved in the solution is simplified. It is more difficult to find a general technique which is helpful in answering the second question: However, there are certain special situations (e.g. rotationally symmetric problems) where the shape of the deformable region can easily be determined.

The purpose of this work is to determine to what extent the techniques of solving structural problems must be modified when using the Coulomb yield criterion, which is linearly dependent on mean stress, together with its associated flow rule which predicts dilatation of the

plastic material. Also, the effect of these material properties on the stresses, velocities, size and shape of the deformable region, etc., will be illustrated by three examples.

First, the limit analysis of beams and plates in cylindrical bending will be considered. The analysis will involve only the axial stress in the beam and therefore, the tensile and compressive yield stresses will be sufficient to describe the yielding process. Therefore, the results of this analysis will be valid for any yield criterion which predicts a different yield stress in tension and compression independent of what the criterion predicts for more complicated stress states. The Coulomb yield criterion is only one example of a yield criterion which has this property. The inherent simplicity of the yielding process in a beam allows one to gain an insight into some of the effects of mean stress as a preparation for considering more complex problems. In this analysis the yield surface for a beam of rectangular cross-section will be found in terms of the moment and axial force. This yield surface will be used to determine the limit load for two beams with different end conditions. The first beam considered will be loaded by a concentrated force at the center and restrained from rotation, but not extension, at both ends. Secondly, a beam will be considered in which the ends are restrained from both rotational and extensional motions. The limit loads will be obtained for each case: They will differ because the tensile and compressive yield stresses are different.

Second, a limit analysis of a cylindrical shell will be considered. In this problem all aspects of the Coulomb yield criterion and its flow rule will be utilized. The analysis will be concerned with both the regular regimes (i.e. flats) and singular regime (i.e. corners) of the Coulomb yield surface. Also, the flow rule will be used and therefore, the additional difficulty of dilatation of the plastic material will be encountered.

The yield surface for a cylindrical shell will be found in terms of the longitudinal and circumferential normal stress resultants and the longitudinal moment. This yield surface will be used to obtain the limit load for a cylindrical shell loaded by a ring of pressure. Two different cases will be considered. One in which a ring of pressure is applied from the inside and the other with a ring of pressure applied from the outside. The limit loads for the two types of loading will be different as a result of the dependence of the Coulomb yield criterion on mean stress.

Third, the plastic analysis of an annular plate, loaded by in-plane pressure at the inside radius, will be considered. In this analysis, as in that of the cylindrical shell, both the regular and singular regimes of the yield surface will be used together with their associated flow rules. The limit load for the annular plate will be found for all ratios of the outside radius to the inside radius. In addition to the limit load, the stress distribution, velocities, displacements, thickening, and the extent of the deforming region will be

found for finite displacements limited only by the assumption of plane stress.

CHAPTER II

LIMIT ANALYSIS OF BEAMS AND PLATES IN CYLINDRICAL BENDING

In the limit analysis of frames the influence of the axial forces is usually neglected because the limit moment of a section is not significantly reduced by a moderate axial force (E.T. Onat and W. Prager [12]). In the analysis of straight beams no axial force is developed at the limit load. Large axial forces may be developed, even at very moderate deflections if the members are fully constrained axially, by continuing the loading beyond the limit load (R.M. Haythornthwaite [13,14]). These axial forces are developed because of geometry changes which occur during the loading and the load-carrying capacity of the beam is increased because of the axial forces. A similar situation occurs in plates when membrane forces are introduced at loads above the limt load (E.T. Onat and R.M. Haythornthwaite [15]). It is possible to introduce some axial force in a structure at the limit load as has been shown by E.T. Onat and W. Prager [16] who considered the limit analysis of arches and found that the limit load was significantly reduced due to the axial forces. For all of the work discussed above, the material was assumed to have a yield criterion which was independent of mean stress. The development of membrane forces in all of these problems was due to the special geometry before yielding as in the case of the arch or to the changes in geometry which occurred during loading above the limit load.

For the present analysis, a beam will be considered and it will be assumed that the material from which the beam is made has a yield criterion which depends on mean stress, i.e. the compressive yield stress of the material will be assumed to have a greater value than the tensile yield stress. These two yield stresses will completely define the yielding process because only the axial stress on the beam will be considered in this analysis. The results of this analysis will apply to all materials which have a different yield stress in tension and compression independent of the yield criterion needed to analyze more complex stress states.

With appropriate end conditions a beam of this material is found to develop significant axial forces at the limit load. The axial forces will be developed because of the material properties and not because of geometry. Before the solution of a special problem is undertaken the yield curve for the beam must be expressed in terms of the bending moment and axial force.

A. YIELD SURFACE

To find the yield curve in terms of the moment and axial force the beam in Fig. 2-1 is considered. The beam is symmetric about the y axis and the z axis passes through the centroid of the cross-section. The stress-strain diagram for the material is shown in Fig. 2-2. A typical fully plastic stress distribution is shown in Fig. 2-3 and for this stress distribution the moment, M, and the axial force, F, can

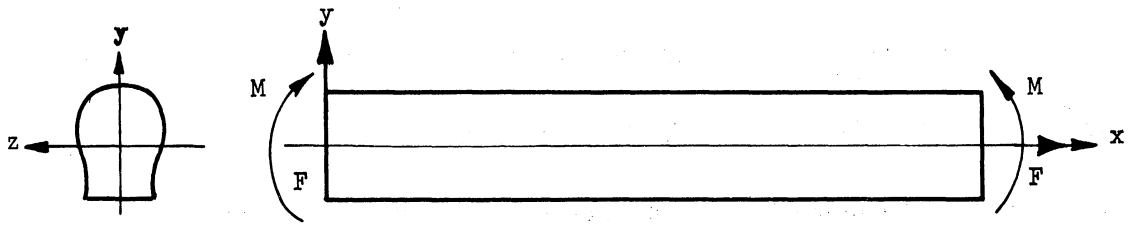

Fig. 2-1. Beam loaded by moment M and axial force F.

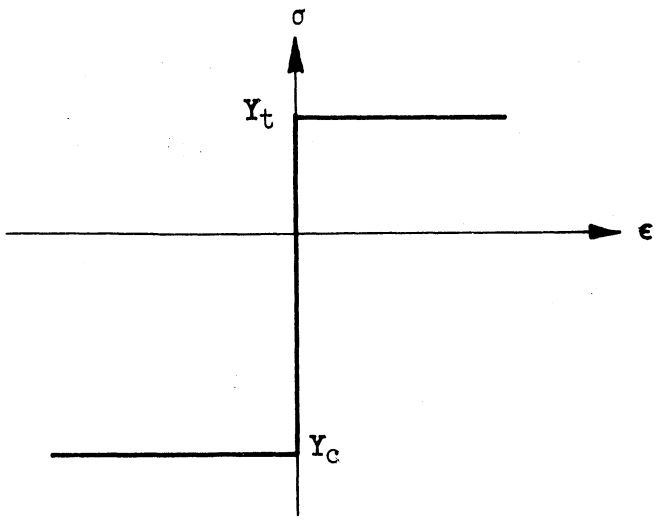

Fig. 2-2. Stress-strain diagram.

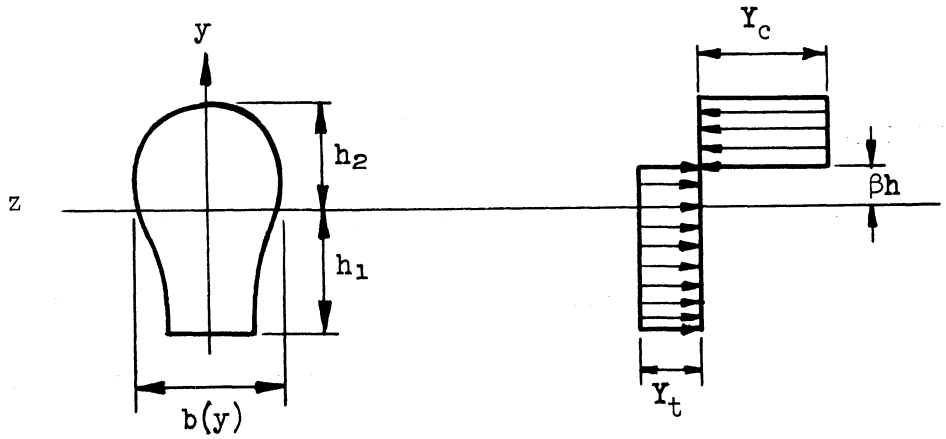

Fig. 2-3. Fully plastic stress distribution in a beam.

be related to the yield stresses, Y_c and Y_t, by the equilibrium equations

$$M = \int_{-h_1}^{\beta h} Y_t b y dy - \int_{\beta h}^{h_2} Y_c b y dy \tag{2.1}$$

and

$$F = \int_{-h_1}^{\beta h} Y_t b dy - \int_{\beta h}^{h_2} Y_c b y dy. \tag{2.2}$$

When $b(y)$ is known, the integrations in Equations (2.1) and (2.2) can be carried out and M can be related to F by eliminating β from Equations (2.1) and (2.2). If a rectangular cross-section is assumed, then $b(y) = b$, $h_1 = h_2 = h/2$, and Equation (2.1) and (2.2) become

$$M = -(\beta h)^2 \frac{b}{2} [Y_t + Y_c] + \frac{bh^2}{2} [Y_t + Y_c] \tag{2.3}$$

and

$$F = \beta bh[Y_t + Y_c] - \frac{bh}{2} [Y_c - Y_t]. \tag{2.4}$$

It will be convenient to make the following changes of variables

$$N^2 |Y_t| = |Y_c| \text{ for } N^2 \geq 1 \tag{2.5}$$

and

$$m = \frac{M}{bh^2 N^2 Y_t}, \quad f = \frac{F}{bhY_t}. \tag{2.6}$$

With these changes in variables, m can be related to f by eliminating β between Equations (2.3) and (2.4):

$$\frac{2mN^2}{(N^2+1)} + f^2 + f(N^2-1) = N^2. \tag{2.7}$$

Equation (2.7) applies for all values of f, but is restricted to $m \geq 0$, in view of the particular stress distribution assumed (see Fig. 2-3).

However, the parallel analysis for the case $m \leq 0$ is straight forward and the entire yield curve can be represented by

$$\frac{2|m|N^2}{(N^2+1)} + f^2 + f(N^2-1) = N^2. \tag{2.8}$$

Equations (2.8) are plotted in Fig. 2-4 for $N^2 = 1$ and $N^2 = 4$. The maximum value of m is given by

$$m_{max} = \frac{(N^2+1)^3}{8N^2} \tag{2.9}$$

and it occurs at

$$f = \frac{1-N^2}{2}. \tag{2.10}$$

When $N^2 = 1$, the yield stresses in tension and compression are equal and there is no influence of mean stress.

Introducing the new variables

$$f' = \frac{2}{N^2+1} f + \frac{N^2-1}{N^2+1}$$

and (2.11)

$$m' = \frac{8N^2}{(N^2+1)^3} m$$

the expression for the yield curve, Equation (2.8), becomes

$$(f')^2 + |m'| = 1. \tag{2.12}$$

This expression may be characterized as the canonical form of the yield curve in the sense that it applies for all criteria for which the yield stresses in tension and compression are different, because the material properties are absorbed in the variables m' and f'. Therefore, Equation (2.12) always has the form shown in Fig. 2-4 with $N^2 = 1$.

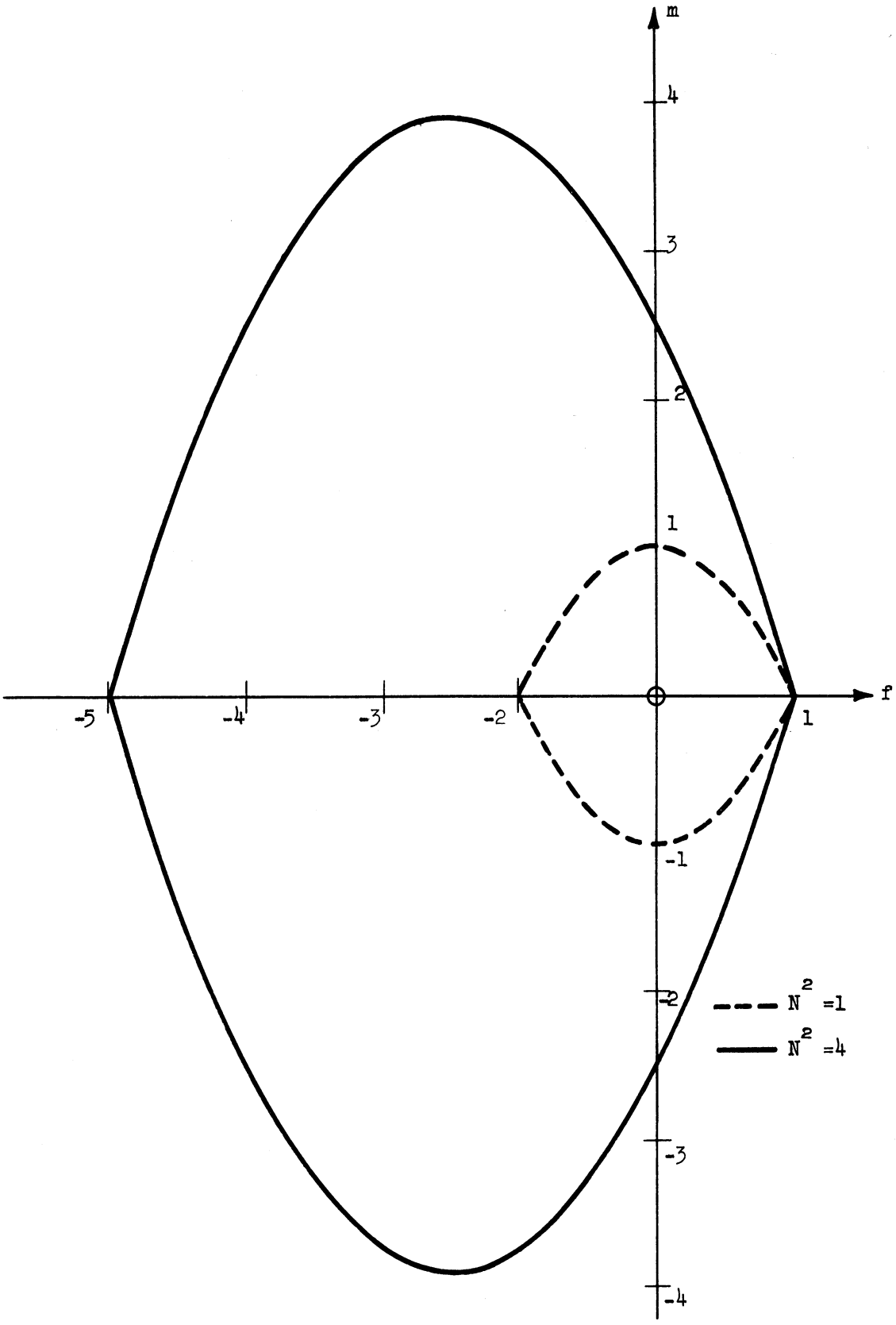

Fig. 2-4. Yield curve for a rectangular beam for $N^2 = 1$ and $N^2 = 4$.

B. SOLUTIONS

Two problems will be considered to show how the end conditions can cause an axial force at the limit load. The first problem will be that of a beam restrained from rotation at the ends and loaded by a concentrated load P at the center as shown in Fig. 2-5. The beam will

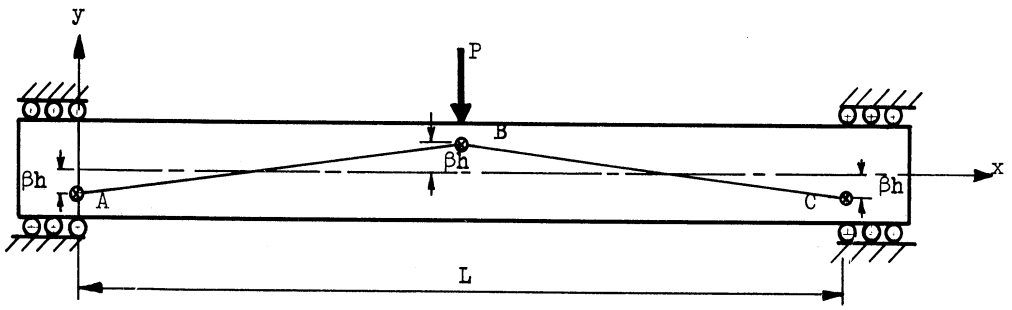

Fig. 2-5. A beam restrained from rotation at the ends and loaded by a concentrated load P at the center.

collapse when hinges have formed at A, B, and C. The hinges at A and C will be associated with the point f = 0, m = $-(1+N^2)/2$ of Fig. 2-4 and the hinge at B will be associated with point f = 0, m = $(1+N^2)/2$ of Fig. 2-4. The hinges will be at a height βh from the x axis. This height can be found by setting F = 0 in Equation (2.4):

$$\beta h = \frac{N^2-1}{2(N^2+1)}\, h. \qquad (2.13)$$

Because these hinges are not co-linear, the beam will fail by both rotation and expansion of the beam. The failure can be understood by imagining that the hinges are connected by rigid bars AB and BC and as the load is increased above the limit load, the end of the beam must move outward. This is consistent with the yield curve of Fig. 2-4 because at the points f = 0 and m = $\pm(1+N^2)/2$ the normal to the yield

curve has a component in the f direction which implies that there must be an axial strain rate in the beam.

From the horizontal equilibrium it is known that the magnitude of F is constant. Therefore from the symmetry of Fig. 2-4 the moments at sections A, B, and C are equal, and the limit load for the beam can then be found from moment equilibrium to be

$$P = \frac{4M_B}{L} . \tag{2.14}$$

In the absence of axial force, the moment M_B at point B of Fig. 2-5 is associated with $m = (1+N^2)/2$ and can be found from Equation (2.6):

$$M_B = \frac{bh^2 Y_t N^2 (1+N^2)}{2} . \tag{2.15}$$

Eliminating M_B from Equations (2.14) and (2.15) gives

$$P = \frac{2bh^2 Y_t (1+N^2)}{L} \tag{2.16}$$

which is the load at which the beam will yield.

However, if the end conditions of Fig. 2-5 are changed so that in addition to there being no rotation, there is also no extensional strain, the beam cannot fail as above. The hinges must move until they are all co-linear and the beam will fail by pure rotation at the ends and under the load. The points of the yield surface that are associated with pure rotation are at the maximum moments. Therefore the equal moments at A, B, and C are found by combining Equations (2.6) and (2.9):

$$M_B = \frac{bh^2Y_t(1+N^2)^3}{8} . \qquad (2.17)$$

Now by eliminating M_B between Equations (2.14) and (2.17) and denoting the load for this case by P_1, it is found that

$$P_1 = \frac{bh^2Y_t(1+N^2)^3}{2L} . \qquad (2.18)$$

Now the ratio P_1/P is given by

$$\frac{P_1}{P} = \frac{(1+N^2)^2}{4N^2} . \qquad (2.19)$$

The axial force associated with P_1 can be found from Equation (2.10) and (2.6):

$$F = \frac{bhY_t(1-N^2)}{2} . \qquad (2.20)$$

Equation (2.19) is shown graphically in Fig. 2-6 to illustrate the increase in the limit load caused by restraining the ends against axial movement.

The results presented here are immediately applicable to the case of rectangular plates supported on two sides and loaded by a line load, parallel to the supported sides, at the mid-span.

Although this analysis does not make use of the Coulomb yield criterion or its flow rule, it does point out some of the effects that can be encountered when using this criterion in more complex analyses such as that for the cylindrical shell which is considered in the next chapter.

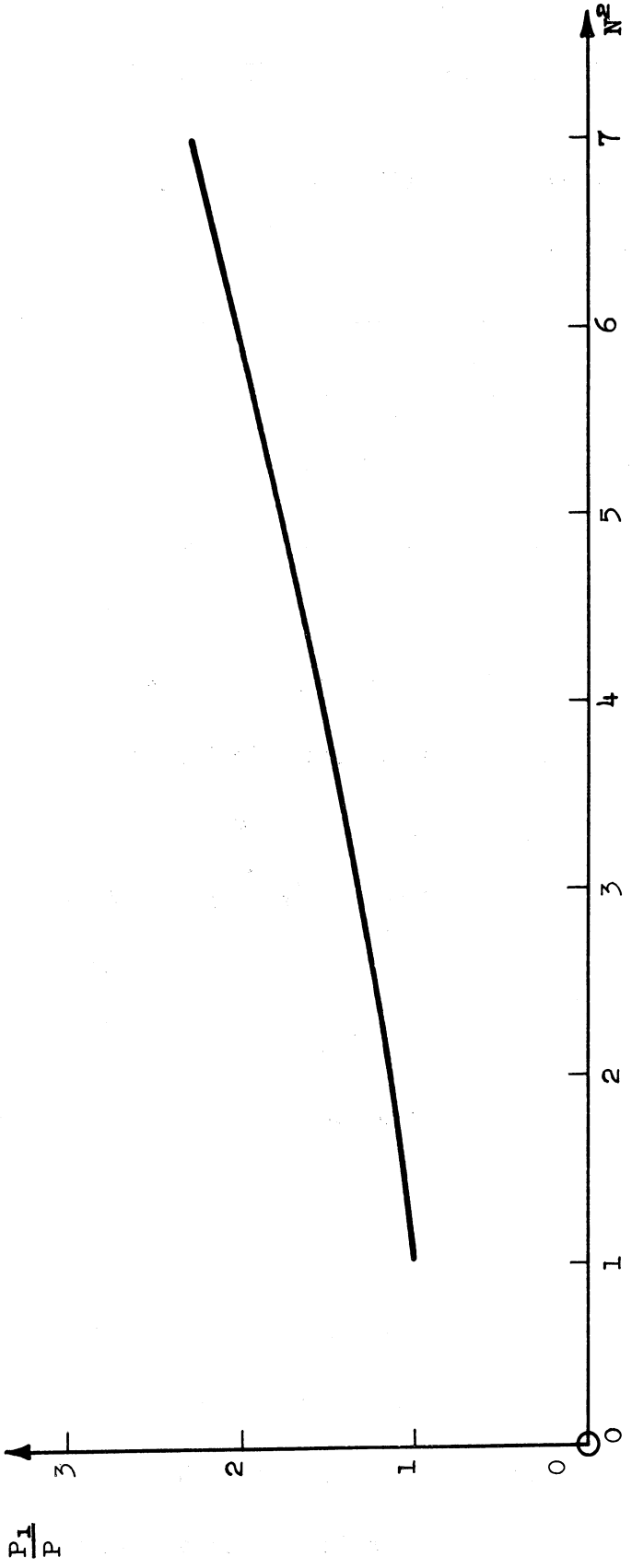

Fig. 2-6. The ratio of the limit loads of a fully restrained beam to a beam restrained from rotation as a function of N^2

CHAPTER III

LIMIT ANALYSIS OF A CYLINDRICAL SHELL

The state of stress in a shell is described by the normal stress resultants, moments, and shear stress resultants. Within the limits of thin-shell theory, transverse shear resultants are considered only in the equations of equilibrium, i.e. there are no strain rates associated with these shear resultants. If the shell and loading are rotationally symmetric, then the principal directions of stress are known and for these directions the twisting moments and in plane shear stress resultants vanish. Thus the state of stress in a thin shell can be defined by four generalized stresses: the principal stress resultants, N_1 and N_2 and the principal moments, M_1 and M_2. For limit analysis problems, the condition of yielding may be represented as a surface in a Cartesian space whose coordinates are the generalized stresses.

Similarly, the strain rate field in a thin shell can be expressed in terms of four generalized strain rates: two principal extensional strain rates, $\dot{e}_1$ and $\dot{e}_2$ and two principal rotation rates $\dot{\kappa}_1$ and $\dot{\kappa}_2$. These strain rates are related to the yield surface by a flow rule which states that the strain rate vector whose components are the generalized strain rates is normal to this surface.

Limit analysis was first applied to shell theory by D.C. Drucker [17], who found the limit load for a long, cylindrical shell loaded by a ring of pressure. This analysis makes use of the Tresca yield

criterion and because there is no axial thrust developed, the yield surface for the shell can be expressed in terms of the longitudinal moment and circumferential normal stress resultant. A linearized version of the yield surface associated with the Tresca yield criterion was used by G. Eason and R.T. Shield [18] for solving problems using a cylindrical shell of any length loaded by a ring of pressure. Further, this problem has been considered by A. Sawczuk and P.G. Hodge, Jr. [19], who compare the limit loads for the yield surfaces of Mises, Tresca, and various linearizations of these.

P.G. Hodge, Jr. [20] and E.T. Onat [21] extended Drucker's work [17] on cylindrical shells to problems in which axial thrust could be developed and used linearized versions of the yield surface expressed in terms of the longitudinal stress resultant, longitudinal moment, and the circumferential moment. A method of obtaining the four dimensional surface for a general shell of revolution by considering all possible strain patterns for an element of the shell was developed by E.T. Onat and W. Prager [22]. They used this method together with the Tresca yield criterion to obtain the yield surface for such a shell. Several approximations to this general yield surface have been introduced by P.G. Hodge, Jr. [23]. The yield surface for a general shell of revolution and a linearized version of it were obtained by P.G. Hodge, Jr. [24] for the Mises yield criterion. D.C. Drucker and R.T. Shield [25] have shown that a good approximation to the yield surface for any shell of revolution can be obtained by using a linearized version of the

yield surface for a cylindrical shell.

In the present work a cylindrical shell which obeys the Coulomb yield criterion and is loaded by a ring of pressure will be considered. The Coulomb yield criterion has been expressed in terms of principal stresses by R.T. Shield [26]. When the yield criterion is viewed in principal stress space, it leads to a yield surface which is an oblate hexagonal pyramid whose axis is the octahedral axis. Because the problem that will be considered here is a problem of plane stress, in cylindrical coordinates, only the plane stress section of this yield surface is presented in Fig. 3-1 (see R.T. Shield [26]).

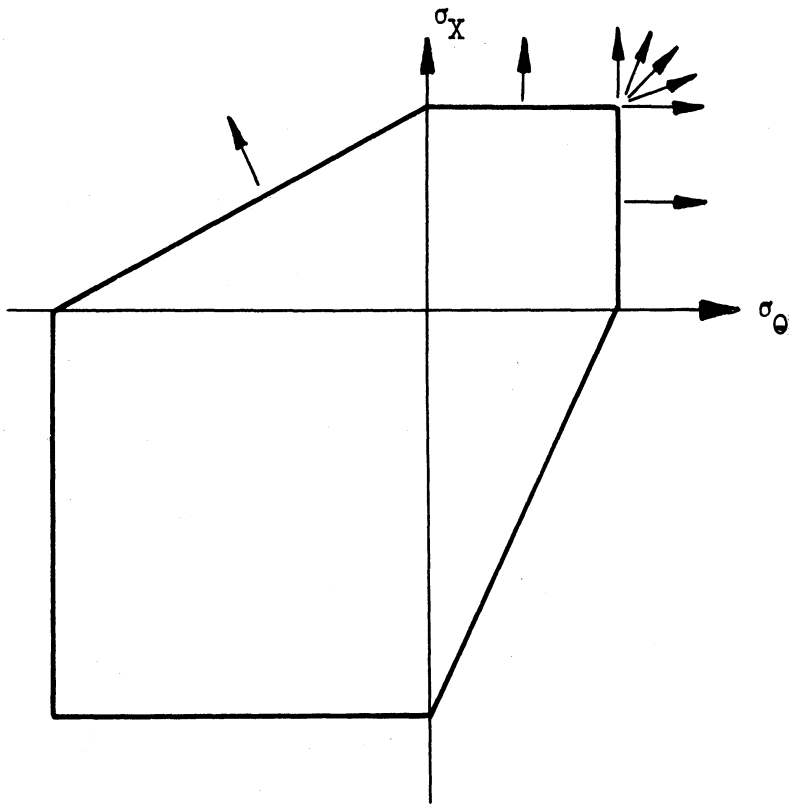

Fig. 3-1. Plane stress section of Coulomb yield criterion.

A. GENERALIZED STRESSES AND STRAIN RATES

Figure 3-2 shows a cylindrical shell element with the stress resultants which act on it. If the loading is axially symmetric, then

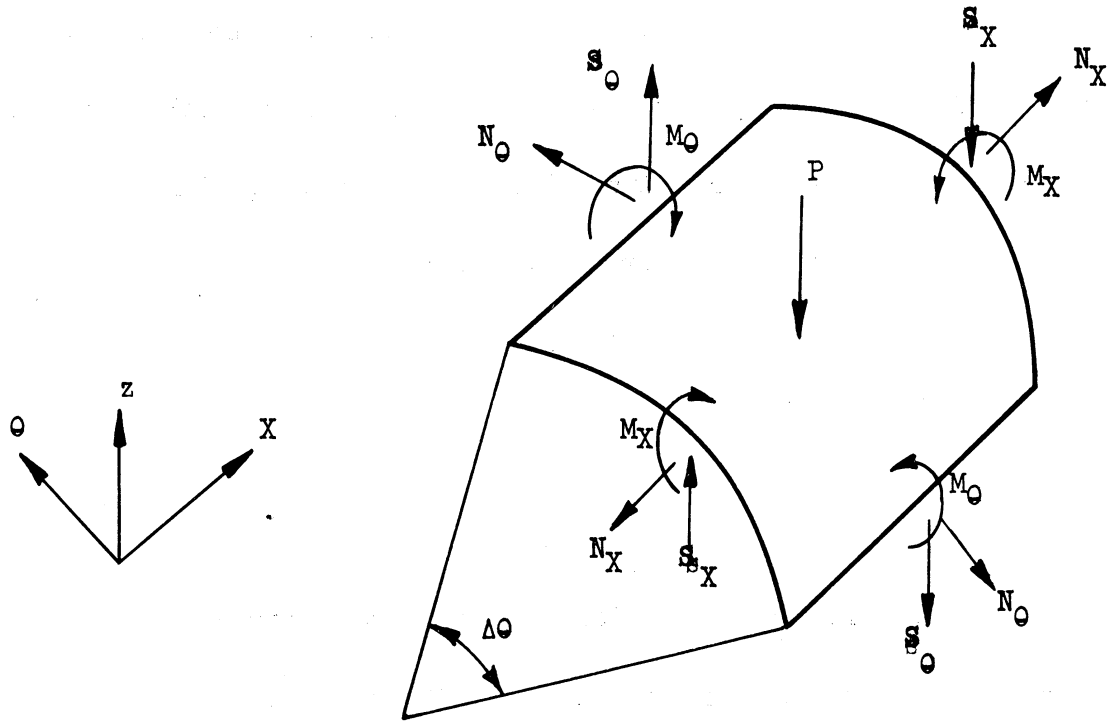

Fig. 3-2. Cylindrical shell element.

the shear resultant S_θ is zero. Also, there is no rotation of the normal in the θ direction and therefore, the moment M_θ does no work and will not appear in the equations for the yield surface. From the usual assumptions for thin shells there is no strain associated with S_X so it becomes a reaction which can be found from equilibrium. Hence S_X will not appear in the formulation of the yield surface. Thus the only generalized stresses which will appear in the expressions for the yield surface are M_X, N_X, and N_θ.

For the velocity field of the plastic flow the usual assumption will be made that the particles originally on the normal to the undeformed middle surface continue to remain on a normal to the middle surface.

The velocity field can be described by the two velocities $\dot{U}$ and $\dot{W}$, where $\dot{U}$ is the velocity in the X direction and $\dot{W}$ is the velocity in the radial direction with the outward direction taken as positive. The strain rates in the middle surface are then

$$\dot{\epsilon}_X = \frac{d\dot{U}}{dX} \tag{3.1}$$

and

$$\dot{\epsilon}_\Theta = \frac{\dot{W}}{R} \tag{3.2}$$

where R is the radius of the middle surface. The rate of change of curvature of the middle surface in the X direction is

$$\dot{\kappa}_X = \frac{d^2\dot{W}}{dX^2} . \tag{3.3}$$

Thus the strain rates throughout the thickness can be written as

$$\dot{e}_\Theta = \frac{\dot{W}}{R} \tag{3.4}$$

and

$$\dot{e}_X = \frac{d\dot{U}}{dX} + z\frac{d^2\dot{W}}{dX^2} \tag{3.5}$$

where z is measured positive outward from the middle surface. The generalized strain rates are $\dot{\epsilon}_X$, $\dot{\epsilon}_\Theta$, and $\dot{\kappa}_X$.

The rate at which energy is dissipated in plastic flow per unit area of the middle surface can be written in terms of the generalized

stresses and strain rates as

$$D = M_X \dot{\kappa}_X + N_X \dot{\epsilon}_X + N_\theta \dot{\epsilon}_\theta . \qquad (3.6)$$

B. YIELD CRITERION AND FLOW RULE

The state of stress at any point of a thin shell is taken to be that of plane stress. Therefore, the plane stress section of the Coulomb yield criterion is shown in Fig. 3-1. For a yield state of stress on a flat side the strain rate vector is normal to that side and at a corner the strain rate vector can be any linear combination with positive coefficients of the strain rate vectors of the adjacent sides.

Inspection of Fig. 3-1 will reveal that when a state of stress is on a flat side the strain rate vector is uniquely determined, but when the stress is in a corner the strain rate vector is not unique. Also if a strain rate vector is given which is associated with a flat side the stress is not uniquely determined but if a strain rate vector is given which is associated with a corner then the state of stress is unique. In spite of the fact that there is no one-to-one correspondence between the yield states of stress and the flow mechanisms the rate d at which energy is dissipated per unit volume is completely determined by the flow mechanism and is given by (See R.T. Shield [26])

$$d = C \cot \phi \, [\dot{e}_1 + \dot{e}_2 + \dot{e}_3] = [|\dot{e}_1| + |\dot{e}_2| + |\dot{e}_3|] C \cos \phi \qquad (3.7)$$

where C is the cohesive strength, ϕ is the angle of friction, and $\dot{e}_1$, $\dot{e}_2$, $\dot{e}_3$ are the principal strain rates. Equation (3.7) can be

written in another form by introducing Y_t, the yield stress in tension, and Y_c the yield stress in compression, where

$$Y_t = 2(\tan(\frac{\pi}{4} - \frac{1}{2}\phi)$$

and

$$Y_c = 2\,C\,\tan\,(\frac{\pi}{4} + \frac{1}{2}\phi).$$

From these definitions it follows that $|Y_c| = N^2|Y_t|$ where $N = \tan(\frac{\pi}{4} + \frac{1}{2}\phi)$. Using these two equations, it is possible to show that

$$2\,C\,\cos\,\phi = \frac{2\,Y_tY_c}{Y_t + Y_c} = \sigma^* \qquad (3.8)$$

where σ^* would be the yield stress in tension and compression if they were equal. Now the energy dissipation per unit volume can be written as

$$d = \frac{\sigma^*}{2}(|\dot{e}_1| + |\dot{e}_2| + |\dot{e}_3|). \qquad (3.9)$$

The three principal strains can be related (see R.M. Haythornthwaite [27]) depending upon the relative values of the strain rates by one of the two equations

$$\dot{e}_\alpha + \dot{e}_\beta + N^2\dot{e}_\gamma = 0 \quad \text{for} \quad e_\alpha \geq 0 \text{ and } e_\beta \geq 0 \qquad (3.10)$$

or

$$\frac{\dot{e}_\alpha}{N^2} + \dot{e}_\beta + \dot{e}_\gamma = 0 \quad \text{for} \quad e_\beta \leq 0 \text{ and } e_\gamma \leq 0 \qquad (3.11)$$

where $\dot{e}_\alpha$, $\dot{e}_\beta$, and $\dot{e}_\gamma$ are the principal strains.*

---

*The subscripts α, β, and γ are used because only the relative values of the principal strain rates are important in these equations and it is impossible to assign say $\dot{e}_1$ to be $\dot{e}_\alpha$ for all cases.

The three principal strain rates for this problem are $\dot{e}_X$, $\dot{e}_\Theta$, and $\dot{e}_Z$. It is possible to express $\dot{e}_X$ and $\dot{e}_\Theta$ in terms of the generalized strain rates as follows

$$\dot{e}_X = \dot{\epsilon}_X + z\dot{\kappa}_X \tag{3.12}$$

and

$$\dot{e}_\Theta = \dot{\epsilon}_\Theta . \tag{3.13}$$

With the aid of Equations (3.10) or (3.11), (3.12), and (3.13) $\dot{e}_Z$ can be expressed in terms of the generalized strain rates.

It is also possible to find the rate of energy dissipation per unit volume in terms of the generalized strain rates from Equation (3.9) and then by integration through the thickness it is possible to find the rate of energy dissipation per unit area of the middle surface. Therefore the result of integrating Equation (3.9) through the thickness must be equivalent to Equation (3.6), and one obtains

$$D = M_X\dot{\kappa}_X + N_X\dot{\epsilon}_X + N_\Theta\dot{\epsilon}_\Theta = \int_{-\frac{h}{2}}^{\frac{h}{2}}[d]dz = \frac{\sigma^*}{2}\int_{-\frac{h}{2}}^{\frac{h}{2}}(|\dot{e}_1|+|\dot{e}_2|+|\dot{e}_3|)dz. \tag{3.14}$$

The right side of Equation (3.14) can be expressed in terms of the generalized strain rates. Typical distributions of the generalized strain rates $\dot{\epsilon}_X$, $\dot{\epsilon}_\Theta$, and $\dot{\epsilon}_Z$ are shown in Fig. 3-3. These distributions are obtained by choosing distributions for $\dot{e}_\Theta$ and $\dot{e}_X$ which are consistant with the assumption that normals remain normal and then finding $\dot{e}_Z$ from either Equation (3.10) or (3.11) depending upon which applies.

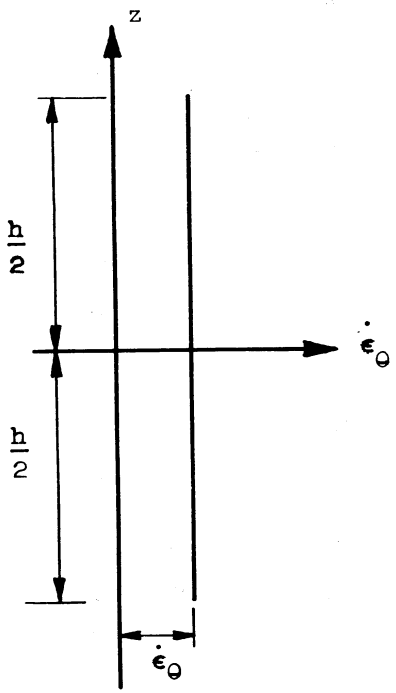

$$|\dot{e}_\theta| = \dot{\epsilon}_\theta$$

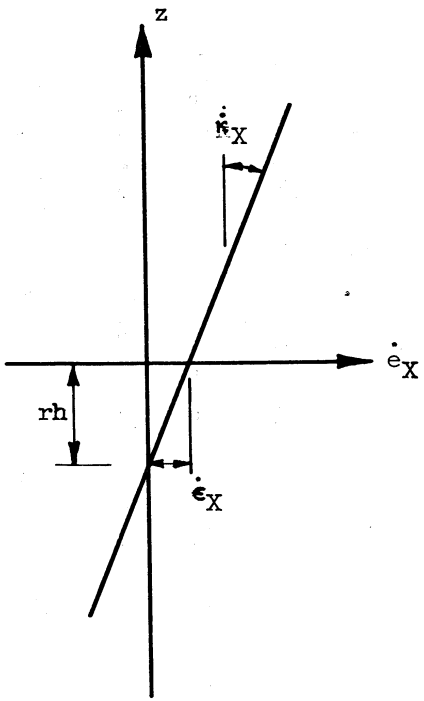

$$|\dot{e}_X| = -(\dot{\epsilon}_X + z\dot{\kappa}_X) \quad \text{for } -\frac{h}{2} \leq z \leq rh$$

$$|\dot{e}_X| = \dot{\epsilon}_X + z\dot{\kappa}_X \quad \text{for } rh \leq z \leq +\frac{h}{2}$$

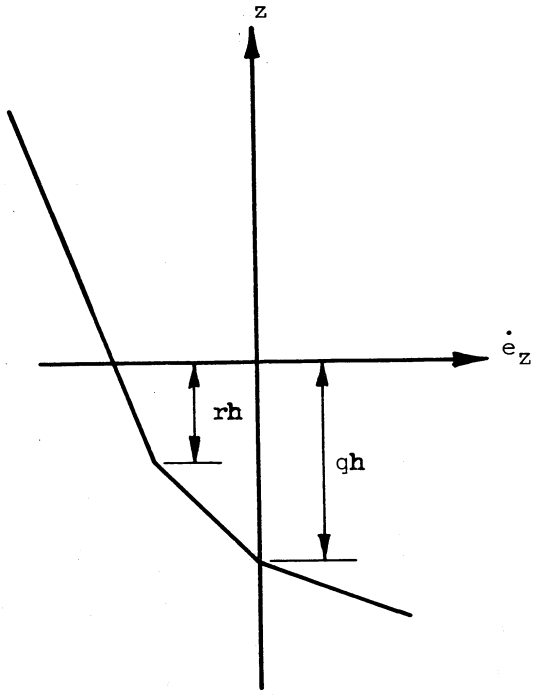

$$|\dot{e}_z| = -(\dot{\epsilon}_\theta + N^2\dot{\epsilon}_X + N^2\dot{\kappa}_X z) \quad \text{for } -\frac{h}{2} \leq z \leq qh$$

$$|\dot{e}_X| = \frac{\epsilon_\theta}{N^2} + \dot{\epsilon}_X + z\dot{\kappa}_X \quad \text{for } qh \leq z \leq rh$$

$$|\dot{e}_z| = \frac{\dot{\epsilon}_\theta + \dot{\epsilon}_X + z\dot{\kappa}_X}{N^2} \quad \text{for } rh \leq z \leq \frac{h}{2}$$

Fig. 3-3. Strain rate distribution in shell element.

Using the distribution of strain rates shown in Fig. 3-3, in Equation (3.14) it is possible to write

$$\frac{2D}{\sigma^*} = \int_{-\frac{h}{2}}^{\frac{h}{2}} \dot{\epsilon}_\Theta dz - \int_{-\frac{h}{2}}^{rh} (\dot{\epsilon}_X + z\dot{\kappa}_X) dz + \int_{rh}^{\frac{h}{2}} (\dot{\epsilon}_X + z\dot{\kappa}_X) dz - \int_{-\frac{h}{2}}^{qh} (\dot{\epsilon}_\Theta + N^2\dot{\epsilon}_X + zN^2\dot{\kappa}_X) dz$$

$$+ \int_{qh}^{rh} (\frac{\dot{\epsilon}_\Theta}{N^2} + \dot{\epsilon}_X + z\dot{\kappa}_X) dz + \frac{1}{N^2} \int_{rh}^{\frac{h}{2}} (\dot{\epsilon}_\Theta + \dot{\epsilon}_X + z\dot{\kappa}_X) dz. \tag{3.15}$$

Carrying out the integrations in Equation (3.15) and then comparing the coefficients of the generalized strain rates of Equation (3.15) with those in Equation (3.6) the stress resultants can be written as

$$N_\Theta = \frac{\sigma^* h(1+N^2)}{2N^2} [-q + \frac{1}{2}],$$

$$N_X = \frac{\sigma^* h(1+N^2)}{2N^2} [-r - N^2 q + \frac{1}{2}(1-N^2)], \tag{3.16}$$

and

$$M_X = \frac{\sigma^* h^2(1+N^2)}{8N^2} [-2r^2 - 2N^2 q^2 + \frac{1}{2}(1+N^2)].$$

In the following the bending moments and the normal stress resultants will be made dimensionless by dividing them by $M_0 = \sigma^* h^2(1+N^2)/8N^2$ and $N_0 = \sigma^* h(1+N^2)/2N^2$, respectively. The notation m_X, n_X, and n_Θ will be used for the dimensionless quantities. Therefore, Equations (3.16) can be written as

$$n_\Theta = -q + \frac{1}{2},$$

$$n_X = -r - N^2 q + \frac{1}{2}(1-N^2), \tag{3.17}$$

and

$$m_X = -2r^2 - 2N^2 q^2 + \frac{1}{2}(1+N^2).$$

Equations (3.17) are a parametric representation of one part of the yield surface for a cylindrical shell (face 2 of Table I). The equations do not represent the entire yield surface because they were derived for a particular flow mechanism (that shown in Fig. 3-3). Equations (3.17) are valid when

$$-\frac{1}{2} \leq q < r \leq \frac{1}{2}. \tag{3.18}$$

If r is always associated with the zero of $\dot{e}_X$ and q is associated with the zero of $\dot{e}_z$, there is another flow mechanism for which Equation (3.18) is valid, but which is associated with equations which are different from those in (3.17). This flow mechanism is shown in Fig. 3-4. That part of the yield surface associated with this flow mechanism is given by (face 3 in Table I), i.e.

$$n_\theta = N^2 q - \frac{N^2}{2},$$

$$n_X = N^2 r + q + \frac{1}{2}(1-N^2), \tag{3.19}$$

and

$$m_X = 2N^2 r^2 + 2q^2 - \frac{1}{2}(N^2+1).$$

Two more sets of equations can be derived which are similar to those of Equations (3.17) and (3.19), but they are only valid when

$$-\frac{1}{2} \leq r < q \leq \frac{1}{2}. \tag{3.20}$$

These two faces of the yield surface are given as faces 1 and 4 in Table I.

There are other cases which must be considered. They occur when $q = r$. The equations for faces 5, 6, 7, and 8 in Table I are derived from the equations for faces 1, 2, 3, and 4, respectively by setting q

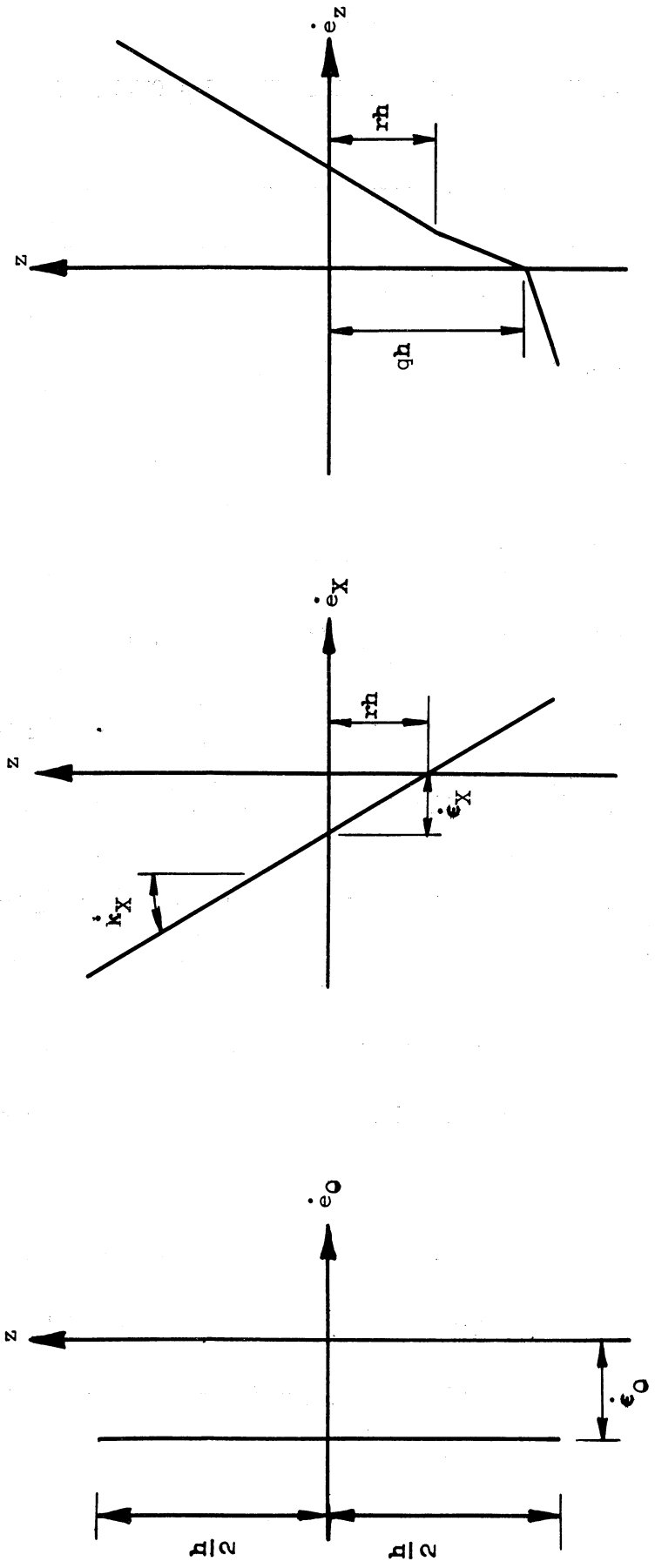

Fig. 3-4. Strain rate distribution in shell element.

TABLE I

PARAMETRIC EQUATIONS OF THE YIELD SURFACE FOR A CYLINDRIAL SHELL

Face	n_θ	n_x	m_x	Inequalities
1	$q + \frac{1}{2}$	$r+N^2q + \frac{1}{2}(1-N^2)$	$2r^2+2q^2N^2 - \frac{1}{2}(N^2+1)$	$-\frac{1}{2} \leq r < q \leq \frac{1}{2}$
2	$-q + \frac{1}{2}$	$-r-N^2q + \frac{1}{2}(1-N^2)$	$-2r^2-2q^2N^2 + \frac{1}{2}(N^2+1)$	$-\frac{1}{2} \leq q < r \leq \frac{1}{2}$
3	$qN^2 - \frac{1}{2}N^2$	$rN^2+q + \frac{1}{2}(1-N^2)$	$2r^2N^2+2q^2 - \frac{1}{2}(1+N^2)$	$-\frac{1}{2} \leq q < r \leq \frac{1}{2}$
4	$-qN^2 - \frac{1}{2}N^2$	$-rN^2-q + \frac{1}{2}(1-N^2)$	$-2r^2N^2-2q^2 + \frac{1}{2}(1+N^2)$	$-\frac{1}{2} \leq r < q \leq \frac{1}{2}$
5	$q + \frac{1}{2}$	$q(1+N^2)+ \frac{1}{2}(1-N^2)$	$2q^2(1+N^2)- \frac{1}{2}(1+N^2)$	$-\frac{1}{2} \leq r = q \leq \frac{1}{2}$
6	$-q + \frac{1}{2}$	$-q(1+N^2) + \frac{1}{2}(1-N^2)$	$-2q^2(1+N^2)+ \frac{1}{2}(N^2+1)$	$-\frac{1}{2} < q = r \leq \frac{1}{2}$
7	$qN^2 - \frac{1}{2}N^2$	$q(1+N^2)+ \frac{1}{2}(1-N^2)$	$2q^2(1+N^2)- \frac{1}{2}(N^2+1)$	$-\frac{1}{2} < q = r \leq \frac{1}{2}$
8	$-qN^2 - \frac{1}{2}N^2$	$-q(1+N^2)+ \frac{1}{2}(1-N^2)$	$-2q^2(1+N^2)+ \frac{1}{2}(1+N^2)$	$-\frac{1}{2} < r = q \leq \frac{1}{2}$

equal to r. This implies that for $z = qh = rh$, $\dot{e}_x = \dot{e}_z = 0$, but from the Equations (3.10) and (3.11) this implies that $\dot{e}_\theta = 0$. Therefore, n_θ does no work.

For faces 1, 2, 3, and 4 it is possible to eliminate q and r from the three parametric equations and obtain one equation in terms of n_θ, n_x, and m_x. These equations are shown as faces 1, 2, 3, and 4 in Table II. Also it is possible to put the inequalities of Table I in terms of n_θ, n_x and m_x these are recorded in Table II.

TABLE II

EQUATION OF THE YIELD SURFACE FOR A CYLINDRICAL SHELL

Face	Yield Surface	Inequalities
1	$m_X-2[n_X-N^2n_Q-\frac{1}{2}(1-2N)]^2-2N^2[n_Q-\frac{1}{2}]^2+\frac{1}{2}(1+N^2)$	$-\frac{1}{2}\leq n_X-N^2n_Q-\frac{1}{2}(1-2N^2)<n_Q-\frac{1}{2}\leq\frac{1}{2}$
2	$-m_X-2[n_X+N^2n_Q+\frac{1}{2}(1-2N^2)]^2-2N^2[\frac{1}{2}-n_Q]^2+\frac{1}{2}(N^2+1)$	$-\frac{1}{2}\leq\frac{1}{2}-n_Q<-n_X+n_QN^2+\frac{1}{2}(1-2N^2)\leq\frac{1}{2}$
3	$m_X-\frac{2}{N^2}[-n_X-\frac{n_Q}{N^2}-\frac{1}{2}(2-N^2)]^2-2[\frac{n_Q}{N^2}+\frac{1}{2}]^2+\frac{1}{2}(N^2+1)$	$-\frac{1}{2}\leq\frac{n_Q}{N^2}+\frac{1}{2}<\frac{n_X}{N^2}-\frac{n_Q}{N^4}-\frac{1}{2N^2}(2-N^2)\leq\frac{1}{2}$
4	$-m_X-\frac{2}{N^2}[-n_X-\frac{n_Q}{N^2}+\frac{1}{2}(2-N^2)]^2-2[\frac{n_Q}{N^2}+\frac{1}{2}]^2+\frac{1}{2}(1+N^2)$	$-\frac{1}{2}\leq\frac{-n_X}{N^2}+\frac{n_Q}{N^4}+\frac{1}{2N^2}(2-N^2)<\frac{n_Q}{N^2}-\frac{1}{2}\leq\frac{1}{2}$
5	$m_X-\frac{2}{1+N^2}[n_X-\frac{1}{2}(1-N^2)]^2+\frac{1}{2}(1+N^2)]$	$-\frac{1}{2}\leq\frac{2n_X-(1-N^2)}{2(1+N^2)}\leq\frac{1}{2}$
6	$-m_X-\frac{2}{1+N^2}[n_X-\frac{1}{2}(1-N^2)]^2+\frac{1}{2}(1+N^2)]$	$-\frac{1}{2}\leq\frac{-2n_X+(1-N^2)}{2(1+N^2)}\leq\frac{1}{2}$

For faces 5, 6, 7, and 8, n_Q cannot appear in the equations of the yield surface because it does no work and therefore q is eliminated between the equations for n_X and m_X. These are shown as faces 5 and 6 in Table II. There are only two faces because ignoring n_Q in faces 5, 6, 7, and 8 of Table I, it is seen that faces 5 and 7 are the same as are faces 6 and 8. It is also possible to express the inequalities for these faces in terms of n_X and these expressions are shown in Table II.

The flow rule can be obtained for each of the faces in Table II and these are shown in Table III. The appropriate inequalities for these faces are also shown.

TABLE III

EQUATIONS OF THE FLOW RULE FOR A CYLINDRICAL SHELL

Face	Flow Rule $\dot{\epsilon}_\theta : \dot{\epsilon}_x : \dot{\kappa}_x$	Inequalities
1	$N^2 4\,[n_x - n_\theta(1+N^2)+N^2] : -4[n_x - N^2 n_\theta - \frac{1}{2}(1-2N^2)] : 1$	$-\frac{1}{2} \leq n_x - N^2 n_\theta - \frac{1}{2}(1-2N^2) < n_\theta - \frac{1}{2} \leq \frac{1}{2}$
2	$N^2 4[n_x - n_\theta(1+N^2)+N^2] : -4[n_x - N^2 n_\theta - \frac{1}{2}(1-2N^2)] : -1$	$-\frac{1}{2} \leq \frac{1}{2} - n_\theta < -n_x + n_\theta N^2 + \frac{1}{2}(1-2N^2) \leq \frac{1}{2}$
3	$\frac{4}{N^6}[N^2 n_x - n_\theta(1+N^2)-N^2] : \frac{-4}{N^2}[n_x - \frac{n_\theta}{N^2} - \frac{1}{2}(2-N^2)] : 1$	$-\frac{1}{2} \leq \frac{n_\theta}{N^2} + \frac{1}{2} < \frac{n_x}{N^2} - \frac{n_\theta}{N^4} - \frac{1}{2N^2}(2-N^2) \leq \frac{1}{2}$
4	$\frac{4}{N^6}[N^2 n_x - n_\theta(1+N^2)-N^2] : \frac{-4}{N^2}[n_x - \frac{n_\theta}{N^2} - \frac{1}{2}(2-N^2)] : -1$	$-\frac{1}{2} \leq \frac{-n_x}{N^2} + \frac{n_\theta}{N^4} + \frac{1}{2N^2}(2-N^2) < \frac{n_\theta}{N^2} - \frac{1}{2} \leq \frac{1}{2}$
5	$0 : \frac{-4}{1+N^2}[n_x - \frac{1}{2}(1-N^2)] : 1$	$-\frac{1}{2} \leq \frac{2n_x - (1-N^2)}{2(1+N^2)} \leq \frac{1}{2}$
6	$0 : \frac{-4}{1+N^2}[n_x - \frac{1}{2}(1-N^2)] : -1$	$-\frac{1}{2} \leq \frac{-2n_x + (1-N^2)}{2(1+N^2)} \leq \frac{1}{2}$

The equations in Table II define a closed convex surface in a stress space which has rectangular Cartesian coordinates n_x, m_x, and n_θ. It is also important to note that as N^2 takes on different values the yield surface for a different material is obtained (i.e. for different values of the ratio of Y_c to Y_t) and the shape of the yield surface will change. Three cross sections of the yield surface for $N^2 = 1$ and $N^2 = 4$ are shown in Figs. 3-5, 3-6, and 3-7. With $N^2 = 1$, this yield surface coincides with the Tresca yield surface and the same three cross sections have been found before (e.g. see E.T. Onat [21]). The effect of mean stress on the yield surface can be seen by comparing the curves for

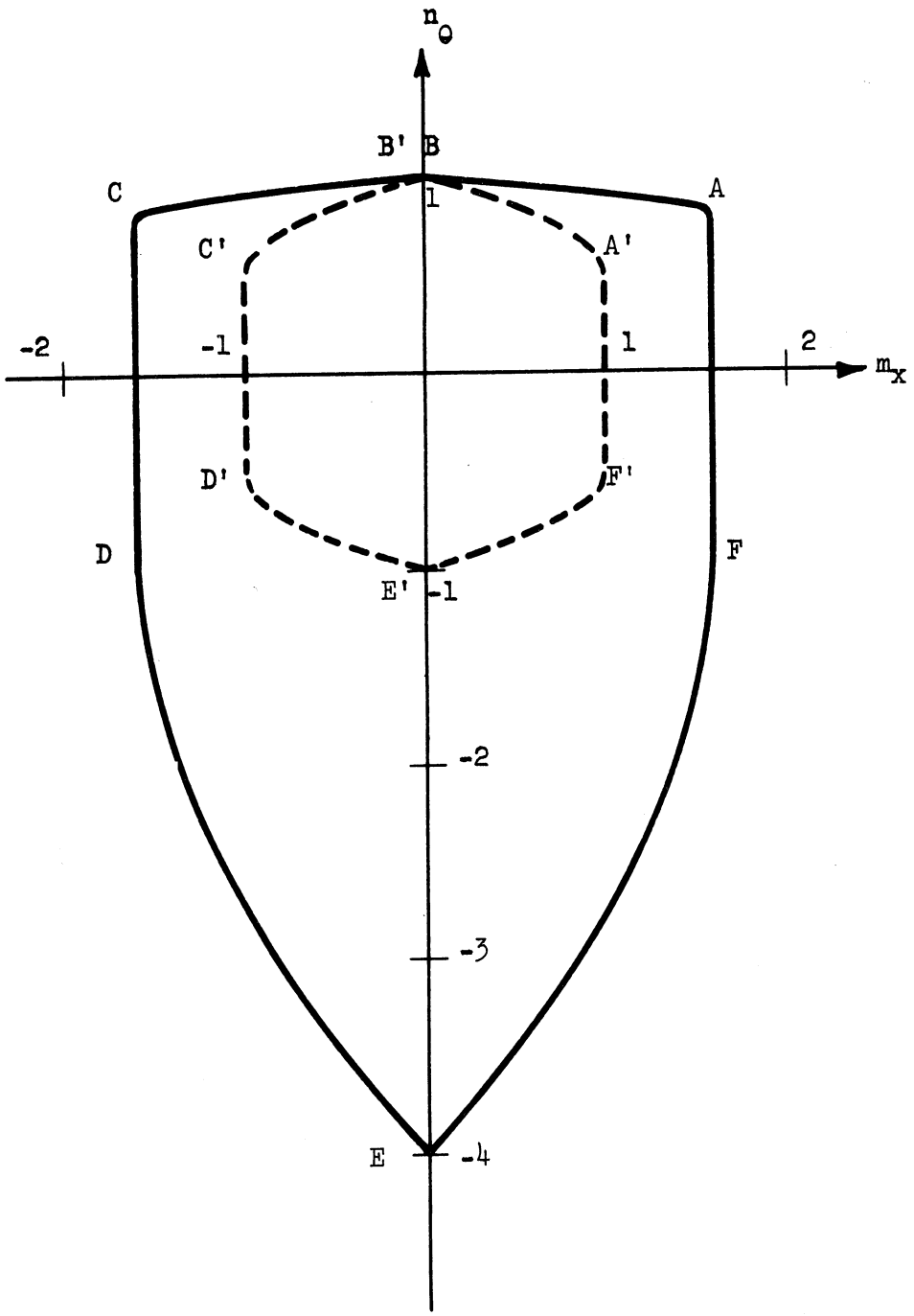

Fig. 3-5. Section of the yield surface for a cylindrical shell with $n_x = 0$ for $N^2 = 1$ and $N^2 = 4$.

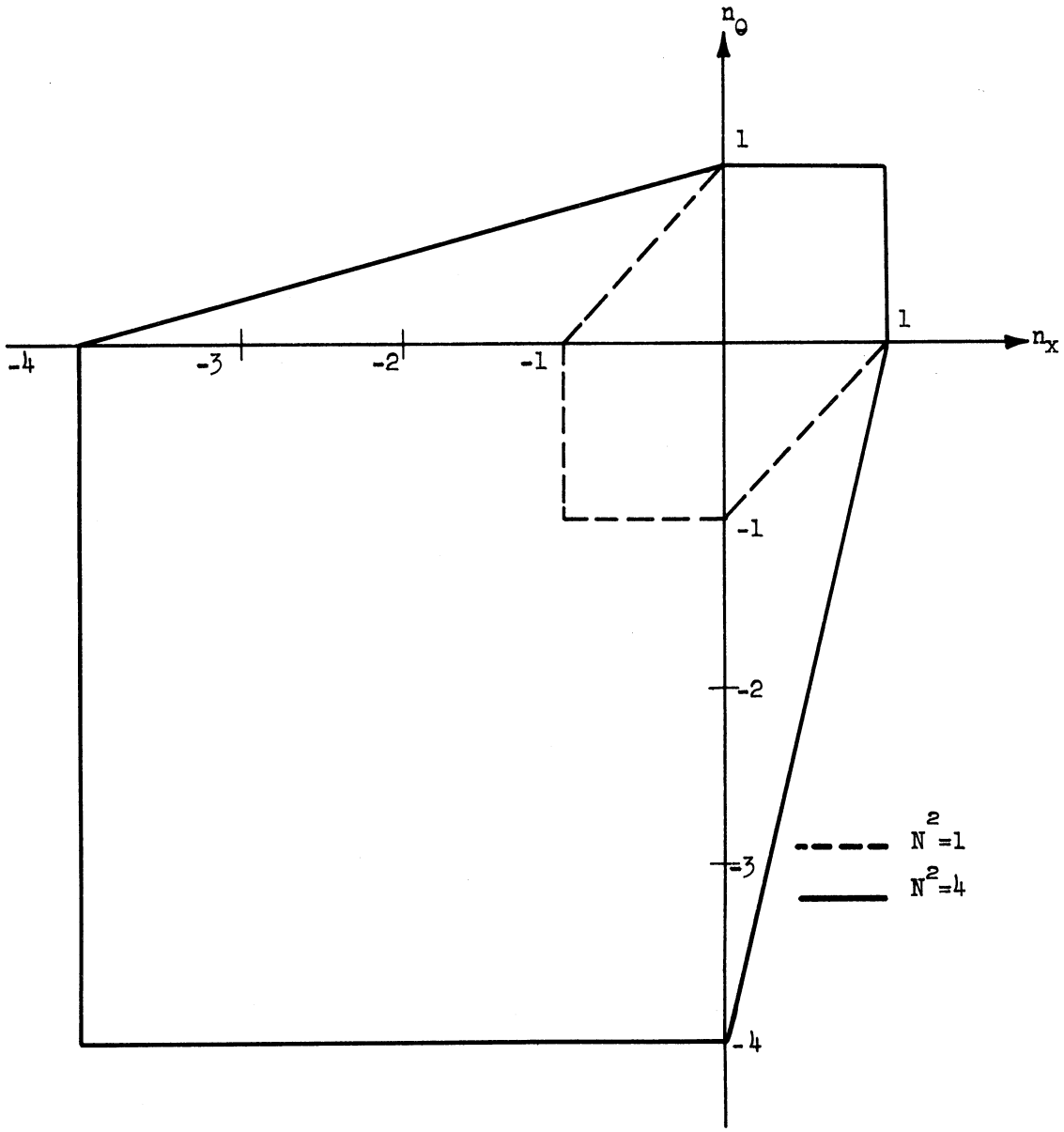

Fig. 3-6. Section of the yield surface for a cylindrical shell with $m_x = 0$ for $N^2 = 1$ and $N^2 = 4$.

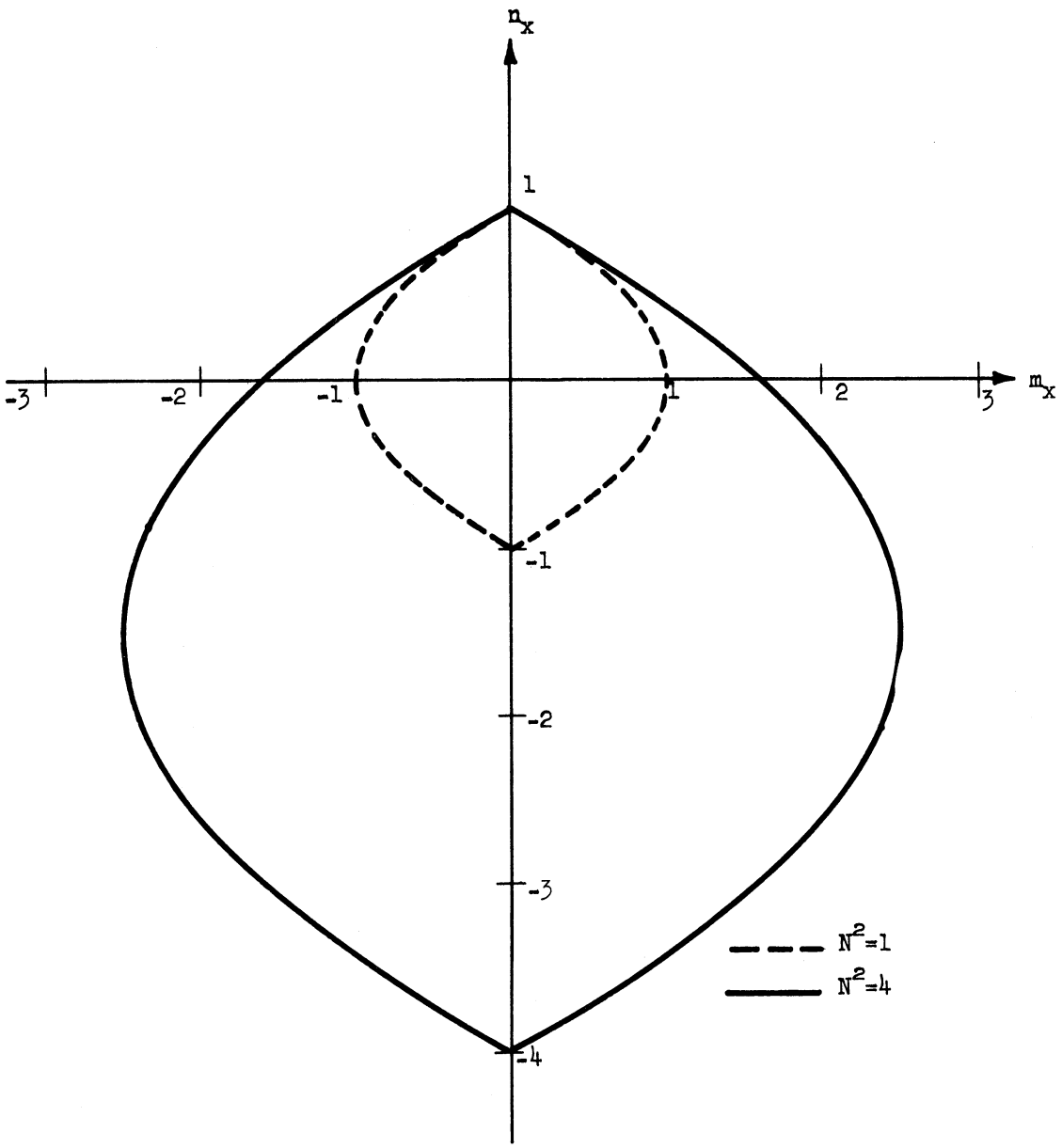

Fig. 3-7. Section of the yield surface for a cylindrical shell with $n_\theta = 0$ for $N^2 = 1$ and $N^2 = 4$.

$N^2 = 1$ with those for $N^2 = 4$. For easy comparison the yield surface has been non-dimensionalized so as to always have the curve pass through unity when n_θ and n_x are positive.

C. ANALYSIS OF A CYLINDRICAL SHELL LOADED WITH A RING OF PRESSURE

The problem to be considered here is that of a long circular cylindrical shell loaded by a ring of pressure as shown in Fig. 3-8.

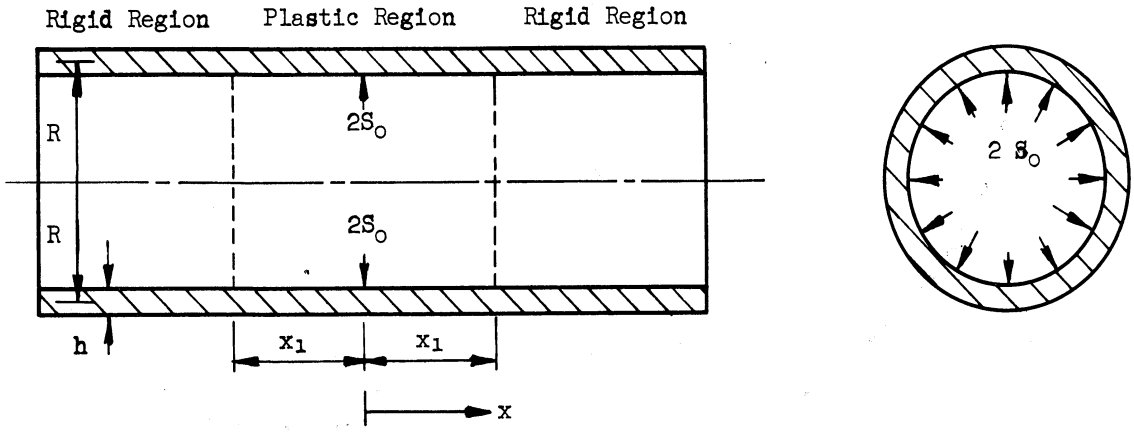

Fig. 3-8. Cylindrical shell loaded by a ring of pressure.

It will be assumed that the shell is long enough so that end effects can be neglected. The problem, then, is to find the extent of the plastic region, the collapse load, and the stresses and velocities in the plastic region. To complete the solution, it will be necessary to find stresses in the rigid region which satisfy the conditions of equilibrium and are at or below yield at every point of the shell.

The behavior of a rigid/perfectly plastic cylindrical shell is governed by two equations of equilibrium, the yield surface, and its associated flow rule. In this problem there is no axial thrust de-

veloped; therefore, the yield surface and flow rule are expressed in terms of n_θ and m_X (see Fig. 3-5).

To obtain the equilibrium equations in non-dimensional form, both the shear stress resultant S_X and the coordinate X must be non-dimensionalized. If this is done by writing

$$s_x = \frac{S_X}{\left(\frac{h}{R}\right)^{1/2} \frac{\sigma^* h(N^2+1)}{4N^2}} \quad \text{and} \quad 2X = x\sqrt{Rh}.$$

the equations of equilibrium can be written as

$$s_x' + n_\theta = 0 \tag{3.21}$$

and

$$m_x' - s_x = 0 \tag{3.22}$$

where the prime denotes differentiation with respect to x.

The two faces of Table I which will be needed are 1 and 2, i.e. regimes AB and BC for $N^2 = 4$ and A'B' and B'C' for $N^2 = 1$ in Fig. 3-5. It will be convenient to use them in parametric form but a change in parameter will be helpful. Since n_θ vanishes in this problem, q and r can be related, and then if $p = q - \frac{1}{2}$, the equations for face 1 become

$$n_\theta = 1 + p$$

and

$$m_x = 2N^2 p[p(1+N^2)+2] \tag{3.23}$$

$$\text{for } -\frac{1}{1+N^2} \leq p \leq 0.$$

For face 2 it is convenient to take $p = q + \frac{1}{2}$ with the results

$$n_\theta = 1 - p$$

and

$$m_x = -2N^2 p[p(1+N^2)-2] \qquad (3.24)$$

$$\text{for } 0 \leq p \leq \frac{1}{1+N^2}.$$

For this problem there are only two generalized strain rates: $\dot{\epsilon}_\theta$ and $\dot{\kappa}_x$ each of which can be expressed in terms of $\dot{W}$. If a dimensionless velocity $\dot{w} = \frac{\dot{W}}{R}$ is introduced then

$$\dot{\epsilon}_\theta = \dot{w} \quad \text{and} \quad \dot{\kappa}_x = \dot{w}''. \qquad (3.25)$$

These are the two components of the strain rate vector which must be normal to the yield surface. The tangent vector has the components dm_x and dn. Therefore, the condition that the strain rate vector be normal to the yield surface is given by

$$\dot{w}'' dm_x + \dot{w} dn_\theta = 0. \qquad (3.26)$$

The two equations of equilibrium (3.21) and (3.22) together with the two faces of the yield surface given by Equations (3.23) and (3.24), and the flow rule expressed in Equation (3.26), will be used in the solution of this problem. The boundary conditions associated with the problem shown in Fig. 3-8 are

$$s_x = s_0 \text{ at } x = 0, \qquad (3.27)$$

$$\dot{w}' = 0 \text{ or a hinge circle exists at } x = 0, \qquad (3.28)$$

$$\dot{w}' = 0 \text{ " " " " " " } x = x_1, \qquad (3.29)$$

and

$$\dot{w} = 0 \text{ at } x = x_1. \qquad (3.30)$$

Because the yield surface has been expressed in parametric form the equilibrium Equations (3.21) and (3.22) can be written as

$$\frac{ds_x}{dp} p' + n_\theta = 0 \tag{3.31}$$

and

$$\frac{dm_x}{dp} p' - s_x = 0. \tag{3.32}$$

Elimination of p' from Equations (3.31) and (3.32) lead to

$$s_x^2 - s_o^2 + 2\int_{p_0}^{p} n_\theta \frac{dm_x}{dp} dp = 0. \tag{3.33}$$

Where p_0 is the value of p at x = 0 and boundary condition (3.27) has been used. Now if s_1 and p_1 are respectively the values of s_x and p at $x = x_1$, Equation (3.33) gives

$$s_o^2 = s_1^2 + 2\int_{p_0}^{p_1} n_\theta \frac{dm_x}{dp} dp. \tag{3.34}$$

It will be shown later that s_x is proportional to $\dot{w}$. Therefore boundary condition (3.30) implies that $s_1 = 0$ and the limit load can be written as

$$s_o = [2\int_{p_0}^{p_1} n_\theta \frac{dm_x}{dp} dp]^{1/2} \tag{3.35}$$

and the shear stress is found to be

$$s_x = [2\int_{p}^{p_1} n_\theta \frac{dm_x}{dp} dp]^{1/2}. \tag{3.36}$$

Since m_x, n_θ, and s_x are known as functions of p, their dependence on x will follow once the functional relation between p and x has been established. This can be accomplished by using Equation (3.32)

$$\frac{dm_x}{dp}\frac{dp}{dx} = s_x$$

and therefore

$$x = \int_{p_0}^{p} \left(\frac{1}{s_x}\right) \frac{dm_x}{dp}\, dp. \tag{3.37}$$

A complete solution for the stresses in the plastic region will be found as soon as p_0 and p_1 are known and they will be determined from the boundary conditions (3.28) and (3.29). However, before this can be done the velocity $\dot{w}$ must be considered. Assuming that p_0 and p_1 are known, the extent x_1, of the plastic region can be written as

$$x_1 = \int_{p_0}^{p_1} \left(\frac{1}{s_x}\right) \frac{dm_x}{dp}\, dp. \tag{3.38}$$

It can be shown that a velocity field of the form

$$\dot{w} = C_1 s_x \tag{3.39}$$

satisfies the requirements of the flow rule expressed in Equation (3.26), which can be written as

$$C_1 s_x'' m_x' + C_1 s_x n_x' = 0.$$

Now substituting m_x' from Equation (3.22) and s_x'' from Equation (3.21) gives

$$- C_1 n_\theta' s_x + C_1 s_x n_\theta' = 0.$$

Therefore, Equation (3.39) for the velocity satisfies Equation (3.26) and all that remains to be considered are the boundary conditions (3.28), (3.29), and (3.30). First, the boundary condition (3.30) gives $s_x = 0$ at $x_1 = 0$ as was assumed above. Now Equations (3.28) and (3.29) imply that

$$C_1 s_x' = 0 \text{ at } x = 0 \text{ and } x = x_1. \tag{3.40}$$

If Equation (3.40) holds, then Equation (3.21) implies that $n_\theta = 0$ at $x = 0$ and $x = x_1$. The two points on the yield surface of Fig. 3-5 for which $n_\theta = 0$ are on flats but on these flats $\dot{\epsilon}_\theta = 0 = \dot{w}$. Since the velocity vanishes this cannot be part of the plastic region. Therefore, Equations (3.28) and (3.29) must be satisfied by having hinge circles at $x = 0$ and $x = x_1$. Hinge circles can be formed at regimes A,A' and C,C' of Fig. 3-5 and the plastic region from $x = 0$ to $x = x_1$ is then associated with regimes AB, BC or A'B', B'C' of Fig. 3-5.

The velocity field is now complete and the stress solution can be completed because p_0 is the value of p associated with points C or C' of Fig. 3-5 and p_1 is the value of p associated with the points A or A' of Fig. 3-5, i.e.

$$p_0 = -\frac{1}{1+N^2} \text{ and } p_1 = \frac{1}{1+N^2}. \tag{3.41}$$

Figure 3-5 is only usable for $N^2 = 4$ or $N^2 = 1$ but Equations (3.41) are valid for all values of N^2. Now that p_1 and p_0 are known, the limit load can be obtained using Equation (3.35). Thus

$$s_0 = \left[2\int_{\frac{-1}{1+N^2}}^{0} (1+p)[4N^2(1+N^2)p+4N^2]dp + 2\int_{0}^{\frac{1}{1+N^2}} (1-p)[-4N^2(1+N^2)p+4N^2]dp \right]^{1/2}$$

or

$$s_0 = \frac{4N}{1+N^2}\left[\frac{3N^2+2}{6}\right]^{1/2}. \tag{3.42}$$

The value of the shear stress s_x can be found as a function of p from Equation (3.36):

$$s_x = \left[2 \int_{p}^{\frac{1}{1+N^2}} (1-p)[-4N^2(1+N^2)p+4N^2]dp \right]^{1/2}$$

or

$$s_x = [8N^2\left(\frac{3N^2+2}{6(1+N2)} - \frac{p^3(1+N^2)}{3} + \frac{p^2(2+N^2)}{2} - p\right)]^{1/2} \qquad (3.43)$$

for

$$0 \leq p \leq \frac{1}{1+N^2}$$

and

$$s_x = \left[2 \int_{0}^{\frac{1}{1+N2}} (1-p)[-4N^2(1+N^2)p+4N^2]dp + 2 \int_{p}^{0} (1+p)[4N^2(1+N^2)p+4N^2]dp \right]^{1/2}$$

or

$$s_x = \left[8N^2\left(\frac{3N^2+2}{6(1+N^2)^2} - \frac{p^3(1+N^2)}{3} + \frac{p^2(2+N^2)}{2} - p\right)\right]^{1/2} \qquad (3.44)$$

for

$$-\frac{1}{1+N^2} \leq p \leq 0.$$

It is now possible to find x as a function of p from Equation (3.37):

$$x = \frac{2N}{\sqrt{2}} \int_{\frac{-1}{1+N^2}}^{p} \frac{[(1+N^2)p + 1]dp}{\left[\frac{3N^2+2}{6(1+N^2)} - \frac{p^3(1+N^2)}{3} - \frac{p^2(2+N^2)}{2} - p\right]^{1/2}} \qquad (3.45)$$

for

$$-\frac{1}{N^2+1} \leq p \leq 0$$

and

$$x = \frac{2N}{\sqrt{2}} \int_{\frac{-1}{N^2+1}}^{0} \frac{[(1+N^2)p + 1]dp}{\left[\frac{3N^2+2}{6(1+N^2)^2} - \frac{p^3(1+N^2)}{3} - \frac{p^2(2+N^2)}{2} - p\right]^{1/2}}$$

$$+\frac{2N}{\sqrt{2}}\int_{0}^{p}\frac{[-(1+N^2)p+1]dp}{\left[\frac{3N^2+2}{6(1+N^2)^2}-\frac{p^3(1+N^2)}{3}+\frac{p^2(2+N^2)}{2}-p\right]^{1/2}}$$

or

$$x=\frac{2N}{\sqrt{2}}\int_{\frac{-1}{1+N^2}}^{0}\frac{[(1+N^2)p+1]dp}{\left[\frac{3N^2+2}{6(1+N^2)^2}-\frac{p^3(1+N^2)}{3}-\frac{p^2(2+N^2)}{2}-p\right]^{1/2}}$$

$$+2N\sqrt{3}\{(3N^2+2)^{1/2}-[-2(1+N^2)p+3N^2+2]^{1/2}\} \qquad (3.46)$$

for

$$0\leq p\leq\frac{1}{1+N^2}\ .$$

The integrals in Equations (3.45) and (3.46) are elliptic. The functional relation between x and p was established by numerical integration, whereupon m_x, n_θ, s_x, and $\overset{\circ}{w}_x$ were known as functions of x. The extent of the plastic region, x_1, can be found by replacing p by $1/(1+N^2)$ in Equation (3.46). The solution of this problem for the Tresca yield criterion is the special case of the above solution for $N^2 = 1$ (e.g. see [19]).

If the ring of pressure in Fig. 3-8 is given the opposite sign (i.e. if the pressure is directed radially inward), the above analysis will not be applicable. The conditions of equilibrium as expressed in Equations (3.21) and (3.22); the flow rule as expressed in Equation (3.26); and the boundary condition, (3.27), (3.28), (3.29), and (3.30) are all applicable, but instead of using regimes AB and BC of Fig. 3-5,

the regimes which will be needed are DE and EF (also the regimes with the primes may be used).

For regime DE (i.e., face 3 of Table I), it is convenient to introduce $p = q + 1/2$ because then

$$n_\Theta = N^2(p-1)$$

and

$$m_x = 2p[p(\frac{1+N^2}{N^2})-2] \tag{3.47}$$

for

$$0 \leq p \leq \frac{N^2}{1+N^2} .$$

For regime EF (i.e., face 4 of Table I), it is convenient to introduce $p = q - 1/2$ because then

$$n_\Theta = -N^2(p+1)$$

and

$$m_x = -2p[p(\frac{1+N^2}{N^2})+2] \tag{3.48}$$

for

$$-\frac{N^2}{1+N^2} \leq p \leq 0.$$

Following the line of reasoning put forth above, the velocity $\dot{w}$ is given by Equation (3.39), the stress point for $x = 0$ is at regime F and the stress point for $x = x_1$ is at regime D. For these conditions

$$p_0 = -\frac{N^2}{1+N^2}$$

and (3.49)

$$p_1 = \frac{N^2}{1+N^2} .$$

It is now possible to find the limit load s_0 from Equation (3.35) by using Equations (3.47), (3.48), and (3.49):

$$s_o = 2\sqrt{2N}\left[\int_{-\frac{N^2}{1+N^2}}^{0}(p+1)[(\frac{1+N^2}{N^2})p+1]dp + \int_{0}^{\frac{N^2}{1+N^2}}(p-1)[(\frac{1+N^2}{N^2})p-1]dp\right]^{1/2}$$

or

$$s_o = \frac{4N^2}{(1+N^2)}\left[\frac{2N^2+3}{6}\right]^{1/2}. \qquad (3.50)$$

The value of the shear stress s_x can be found as a function of p from Equation (3.36) using Equations (3.47), (3.48), and (3.49):

$$s_x = 2\sqrt{2N}\left[\int_{p}^{\frac{N^2}{1+N^2}}(p-1)[(\frac{1+N^2}{N^2})p-1]dp\right]^{1/2}$$

or

$$s_x = 2\sqrt{2}\left[\frac{N^4(2N^2+3)}{6(1+N^2)^2} - \frac{p^3(1+N^2)}{3} + \frac{p^2(2N^2+1)}{2} - N^2p\right]^{1/2} \qquad (3.51)$$

for

$$0 \le p \le \frac{N^2}{1+N^2}$$

and

$$s_x = 2\sqrt{2N}\left[\int_{p}^{0}(p+1)[(\frac{N^2+1}{N^2})p+1]dp + \int_{0}^{\frac{N^2}{1+N^2}}(p-1)[(\frac{N^2+1}{N^2})p-1]dp\right]^{1/2}$$

or

$$s_x = 2\sqrt{2}\left[\frac{N^4(2N^2+3)}{6(1+N^2)^2} - \frac{p^3(1+N^2)}{3} - \frac{p^2(2N^2+1)}{2} - N^2p\right]^{1/2} \qquad (3.52)$$

for

$$-\frac{N^2}{1+N^2} \le p \le 0.$$

It is now possible to find x as a function of p from Equation (3.37):

$$x = \frac{2}{\sqrt{2}}\int_{-\frac{N^2}{N^2+1}}^{p}\frac{[(\frac{N^2+1}{N^2})p + 1]dp}{\left[\frac{N^2(2N^2+3)}{6(1+N^2)^2} \quad \frac{p^3(1+N^2)}{3} \quad \frac{p^2(2N^2+1)}{2} - N^2p\right]^{1/2}} \qquad (3.53)$$

for

$$-\frac{N^2}{N^2+1} \leq p \leq 0$$

and

$$x = \frac{2}{\sqrt{2}} \int_{-\frac{N^2}{N^2+1}}^{0} \frac{[(\frac{N^2+1}{N^2})p+1]dp}{\left[\frac{N^4(2N^2+3)}{6(1+N^2)^2} - \frac{p^3(1+N^2)}{3} - \frac{p^2(2N^2+1)}{2} - N^2p\right]^{1/2}}$$

$$+\frac{2}{\sqrt{2}} \int_{0}^{p} \frac{[(\frac{N^2+1}{N^2})p-1]dp}{\left[\frac{N^4(2N^2+3)}{6(1+N^2)^2} - \frac{p^3(1+N^2)}{3} + \frac{p^2(2N^2+1)}{2} - N^2p\right]^{1/2}}$$

or

$$x = \frac{2}{\sqrt{2}} \int_{-\frac{N^2}{N^2+1}}^{0} \frac{[(\frac{N^2+1}{N^2})p+1]dp}{\left[\frac{N^4(2N^2+3)}{6(1+N^2)^2} - \frac{p^3(1+N^2)}{3} - \frac{p^2(2N^2+1)}{2} - N^2p\right]^{1/2}}$$

$$+\frac{2\sqrt{3}}{N^2}\{[2N^2+3]^{1/2} - [-2p(1+N^2)+2N^2+3]^{1/2}\} \qquad (3.54)$$

$$0 \leq p \leq \frac{N^2}{1+N^2} .$$

The elliptic integrals in Equations (3.53) and (3.54) were evaluated by numerical integration to complete the solution.

D. NUMERICAL RESULTS

To illustrate the differences in the load carrying capacity of the shell when the loading is either negative or positive, Equations (3.42) and (3.50) are plotted in Fig. 3-9. The limit load is a function of the material property N^2 as well as the type of loading. If the shell

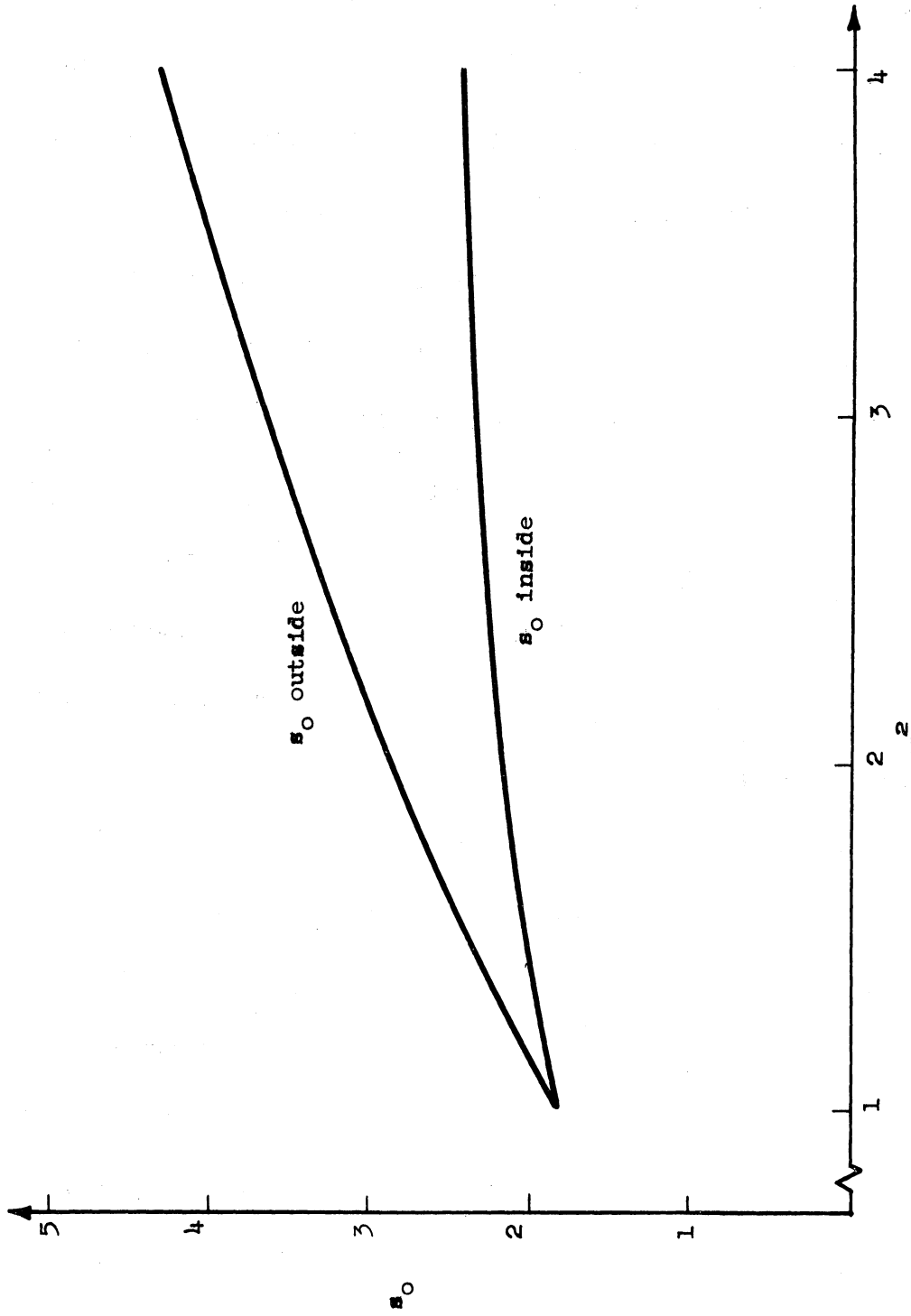

Fig. 3-9. Limit load as a function of N^2.

is loaded by an internal pressure, the limit load is given by Equation (3.42) and as is seen in Fig. 3-9 the limit load increases with the increasing values of N^2. When the load is an external pressure, the limit load also increases with increasing N^2 as given by Equation (3.50) in Fig. 3-9. However, the most important result shown in Fig. 3-9 is that the limit load associated with an external pressure is larger than that associated with an internal pressure for all values of $N^2 > 1$ (for $N^2 = 1$ the Coulomb yield criterion coincides with the Tresca yield criterion and no dependence on the type of loading should be expected). The dependence of the limit load on the type of loading can best be understood by noting that an external ring of pressure causes the circumferential normal stress resultant to be negative and for a material which obeys the Coulomb yield criterion the compressive yield stress is greater than the tensile yield stress.

When the numerical integration in Equations (3.45) and (3.46) are carried out, p is known as a function of x for the case of an internal ring of pressure. With these results the moment m_x and the normal stress resultant n_θ are known as functions of x from Equations (3.23) and (3.24), the shear stress resultant s_x is known from Equations (3.43) and (3.44), and the radial velocity $\dot{w}$ is known from Equation (3.39). For the case of internal loading m_x has been plotted in Fig. 3-10, $-n_\theta$ plotted in Fig. 3-11, and $-s_x$; $-\dot{w}$ plotted in Fig. 3-12. When the numerical integrations in Equations (3.53) and (3.54) are carried out, p is known as a function of x for the case of external loading. From

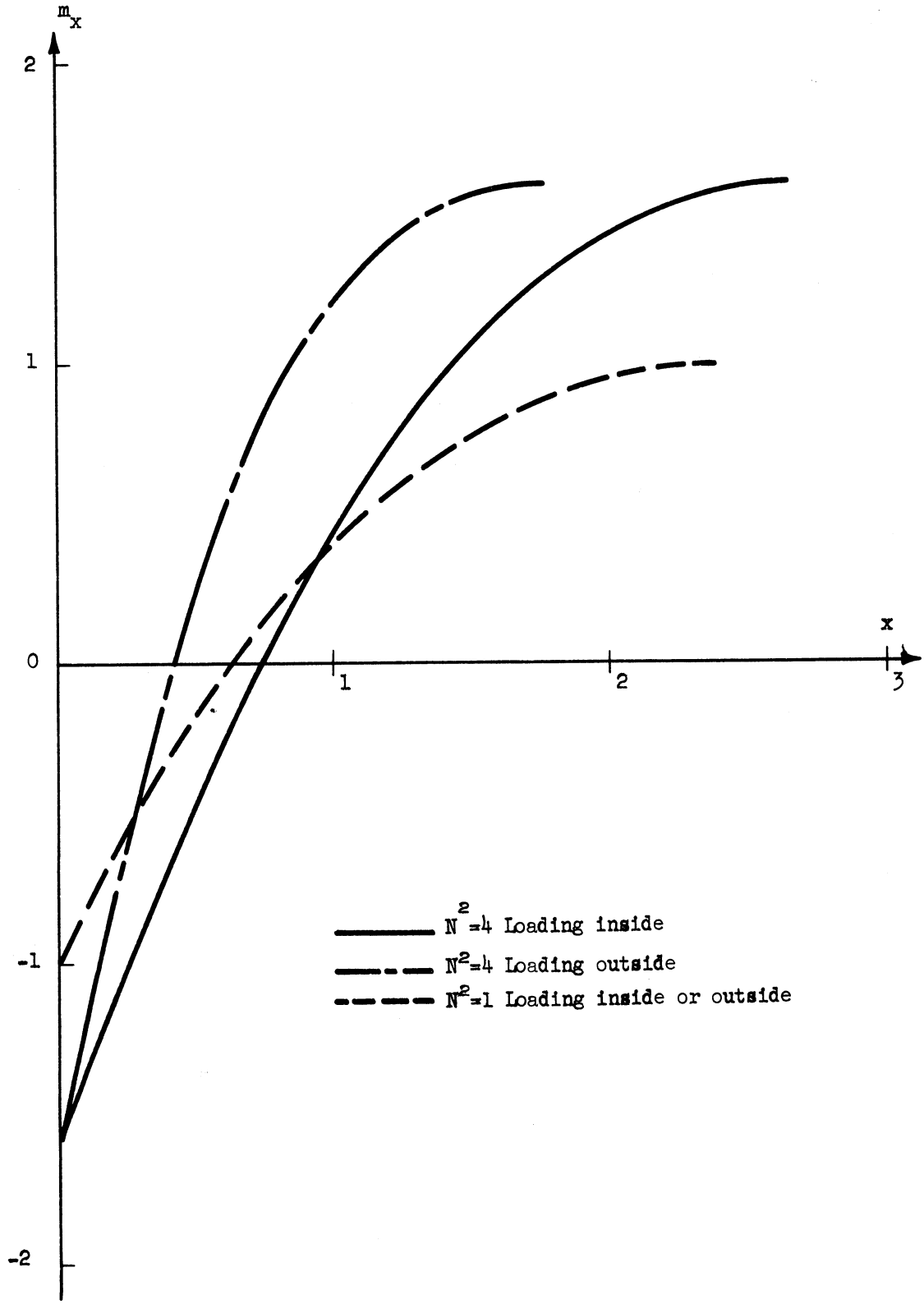

Fig. 3-10. Longitudinal moment as a function of distance.

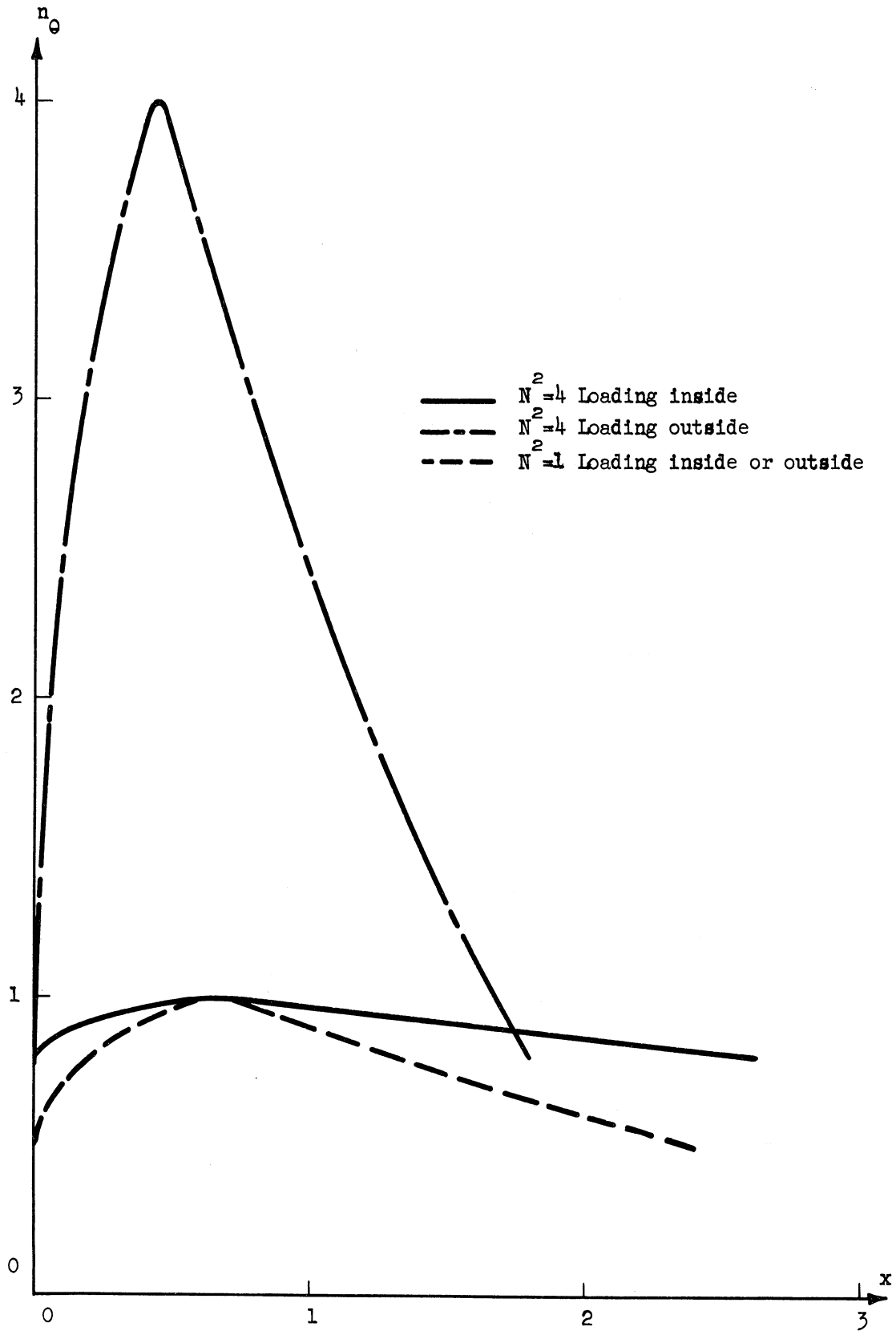

Fig. 3-11. Circumferential normal stress resultant as a function of distance.

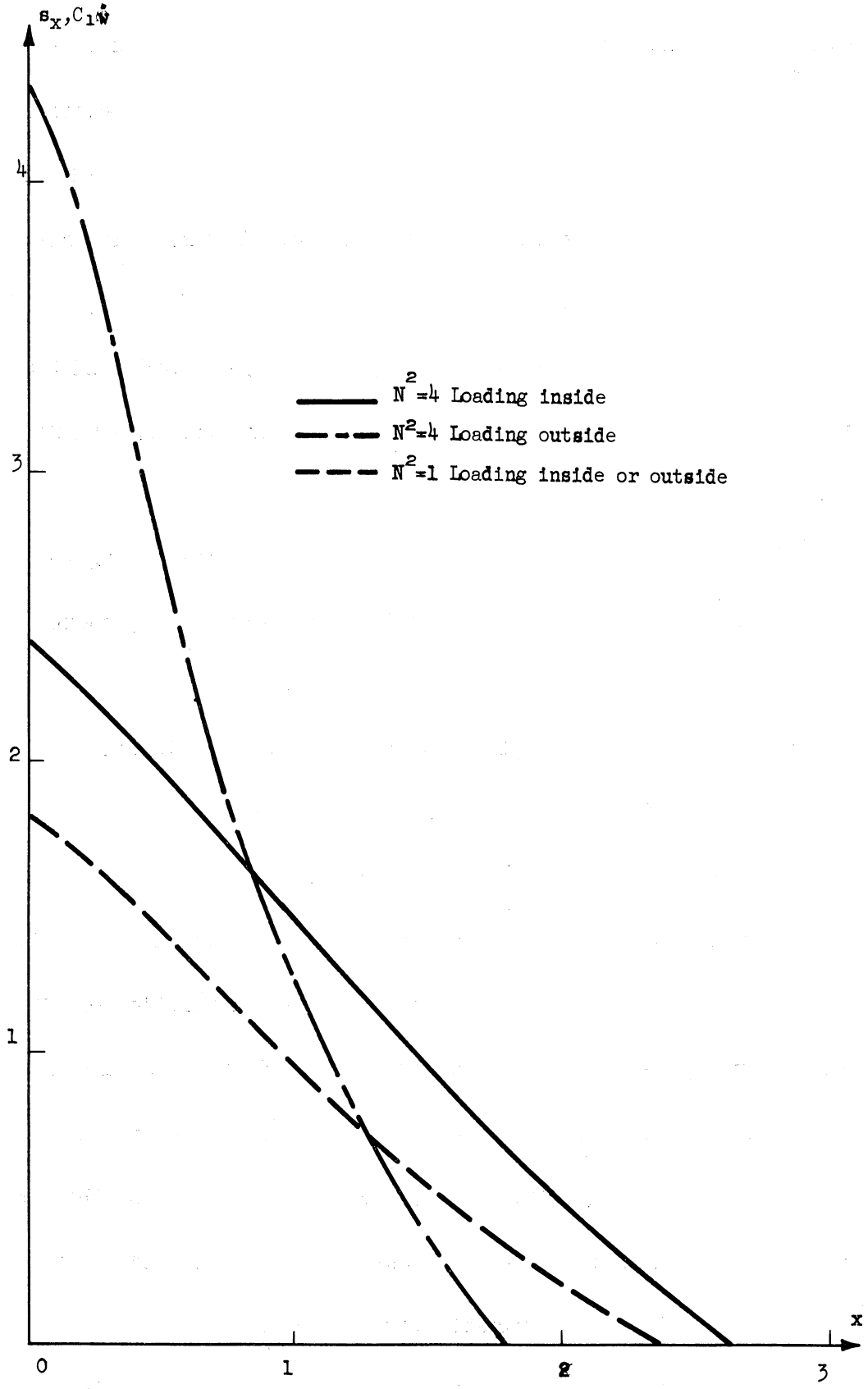

Fig. 3-12. Longitudinal shear stress resultant or radial velocity as a function of distance.

these results it is possible to find m_x and n_θ from Equations (3.47) and (3.48), s_x from Equations (3.51) and (3.52); and $\dot{w}$ from Equation (3.39). These results are plotted in Figs. 3-10, 3-11, and 3-12 for easy comparison with the results for the internal loading. To make it more convenient to compare the results $-m_x$ is plotted in Fig. 3-10 for the case of external loading. In Figs. 3-10, 3-11, and 3-12 the results would be the same for both internal and external loading for $N^2 = 1$.

For the numerical cases considered above, it is interesting to compare the relative sizes of the plastic region given by x_1 shown in Fig. 3-8:

$x_1 = 2.38$ for $N^2 = 1$ internal or external loading

$x_1 = 2.63$ for $N^2 = 4$ internal loading

$x_1 = 1.79$ for $N^2 = 4$ external loading.

As seen in Fig. 3-9, the limit load for the external loading is higher than that for the internal load and is an increasing function of N^2. The size of the plastic region given by $2x_1$ is a decreasing function of N^2 for external loading and is smaller than that of the plastic region for internal loading. Therefore, the increased value of the limit load comes only from the higher compressive yield stress and not because more material is being plastically deformed.

To complete the solution, a stress field must be found in the rigid region which is at or below yield everywhere and which satisfies equi-

librium. Such a stress field has been illustrated by G. Eason and R.T. Shield [18] for a material which obeys the Tresca yield criterion. The same type of stress field can be found for the problem considered here. A typical stress field is illustrated in Fig. 3-13 for the case of internal loading. The equations for this type of stress field for all values of N^2 are as follows

$$\text{for } x_1 \leq x \leq x_2 = x_1+2,$$

$$s_x = \frac{N^2}{2(1+N^2)}(x_1-x),$$

$$m_x = \frac{N^2}{1+N^2}\left[-\frac{1}{4}(x-x_1)^2+2\right], \qquad (3.55)$$

$$n_\theta = \frac{N^2}{2(1+N^2)},$$

and

$$\text{for } x_1+2 = x_2 \leq x \leq x_3 = x_1+4,$$

$$s_x = \frac{N^2}{2(1+N^2)}(x_1-x_3),$$

$$m_x = \frac{N^2}{1+N^2}\left[\frac{1}{2}(x-x_2)^2-(x-x_2)+1\right], \qquad (3.56)$$

$$n_\theta = \frac{-N^2}{2(1+N^2)},$$

and

$$\text{for } x > x_3 = x_1+4,$$

$$m_x = s_x = n_\theta = 0. \qquad (3.57)$$

Similar equations can be found for the case of external loading.

The entire analysis is now complete because the deforming region has been identified, stress resultants have been found which satisfy

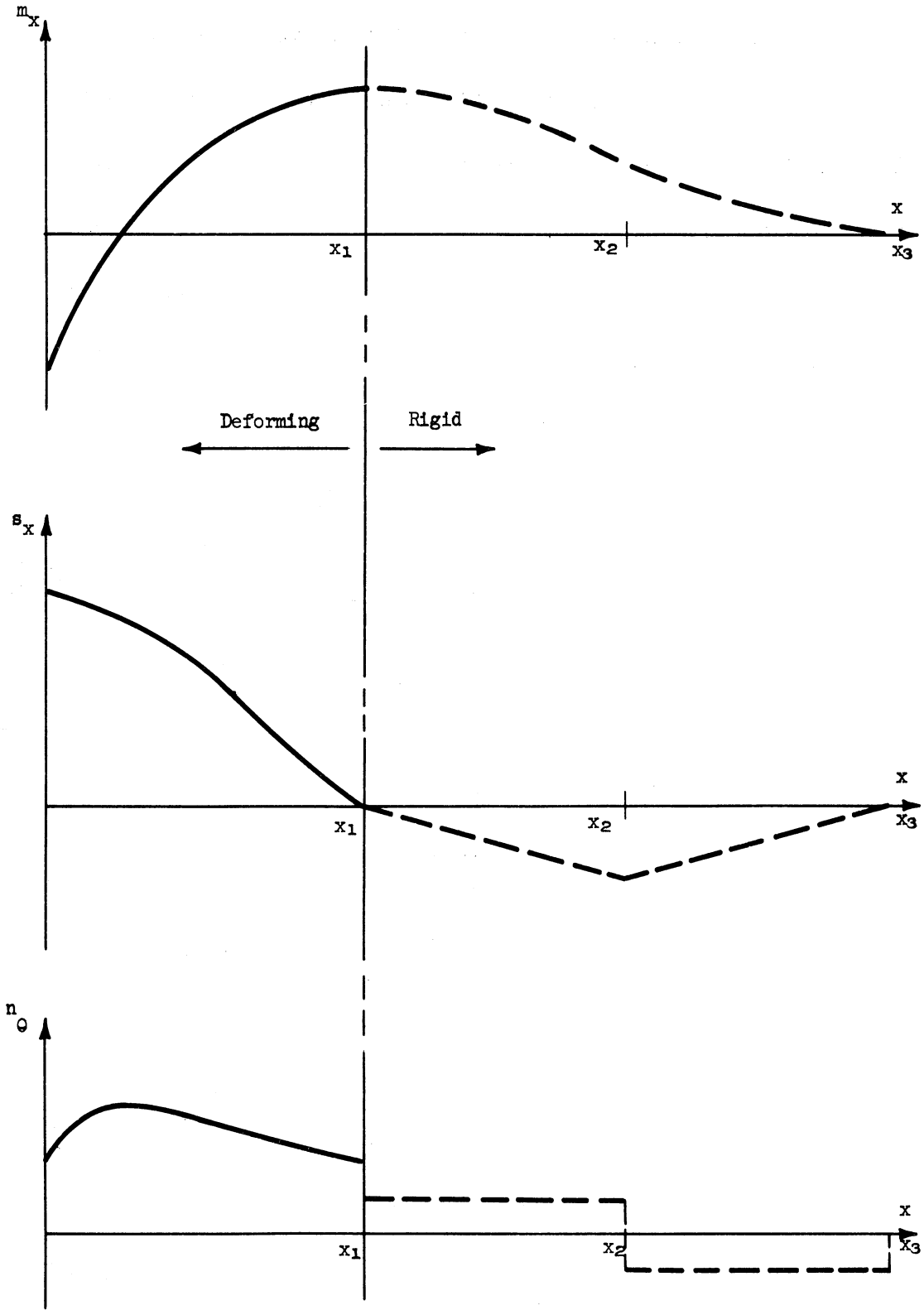

Fig. 3-13. A typical distribution of the stress resultant for internal loading.

equilibrium and the stress boundary conditions, and velocities have been found in the deforming region which are related to the stresses by the flow rule.

CHAPTER IV

PLASTIC ANALYSIS OF AN ANNULAR PLATE

The finite expansion of a hole in a thin infinite plate in a state of plane stress has been investigated for various materials and conditions of loading [28-35]. One solution for a rigid/perfectly plastic plate was obtained by G.I. Taylor [28] and R. Hill [29] using the Tresca yield criterion and the flow rule associated with the Mises yield criterion. W. Prager [30] used the Tresca yield criterion and its associated flow rule to obtain solutions for a rigid/perfectly plastic plate* and for a rigid/plastic plate with isotropic hardening. A limitation on the amount of expansion in Prager's solution for hardening was removed by P.G. Hodge and R. Sankaranarayanan [31]. The expansion problem also has been solved by Sokolovsky [32] for a rigid/perfectly plastic plate using the Mises yield criterion and its associated flow rule. This problem has been combined with the twisting of a plate by R.P. Nordgren and P.M. Naghdi [33]. The finite twisting and expansion of an annular rigid/plastic plate is considered for both the Mises yield criterion and its associated flow rule and for the Tresca yield criterion and its associated flow rule. Numerical results are given which illustrate the influence of twisting on the expansion of a hole in an infinite plate. Also, the expansion problem has been handled by J.M.

*This stress solution was obtained previously by H.A. Bethe without the use of a flow rule. See Taylor [1] and Prager [3].

Alexander and H. Ford [34] for an elastic/plastic plate with isotropic hardening using the Mises yield criterion and its associated flow rule. Another elastic/plastic solution is presented by R.P. Nordgren and P.M. Naghdi [35], in which an annular plate is considered loaded in the plane of the plate with both a pressure and a couple. Using the Tresca yield criterion and its associated flow rule, results are obtained for the elastic/perfectly plastic solutions during both loading and unloading, and work hardening solutions for loading with both isotropic and kinematic hardening. Results are presented for the infinite plate with infinitesimal displacements.

The solution presented here will differ from those mentioned above in that it will be assumed that the plate obeys the Coulomb yield criterion and the flow rule associated with it by the theory of perfectly plastic solids. The plane stress section of the Coulomb yield criterion is shown in Fig. 4-1.

A. BASIC EQUATIONS

This problem will be treated as a problem of plane stress in cylindrical coordinates, i.e. $\sigma_z, \tau_{\theta z}$, and τ_{rz} are taken to be zero and the other stresses are averaged through the thickness. During plastic flow, the thickness in the z direction may not remain uniform but the state of stress may still be approximated as plane if the change in thickness is not too severe. A sketch of the problem is seen in Fig. 4-2a.

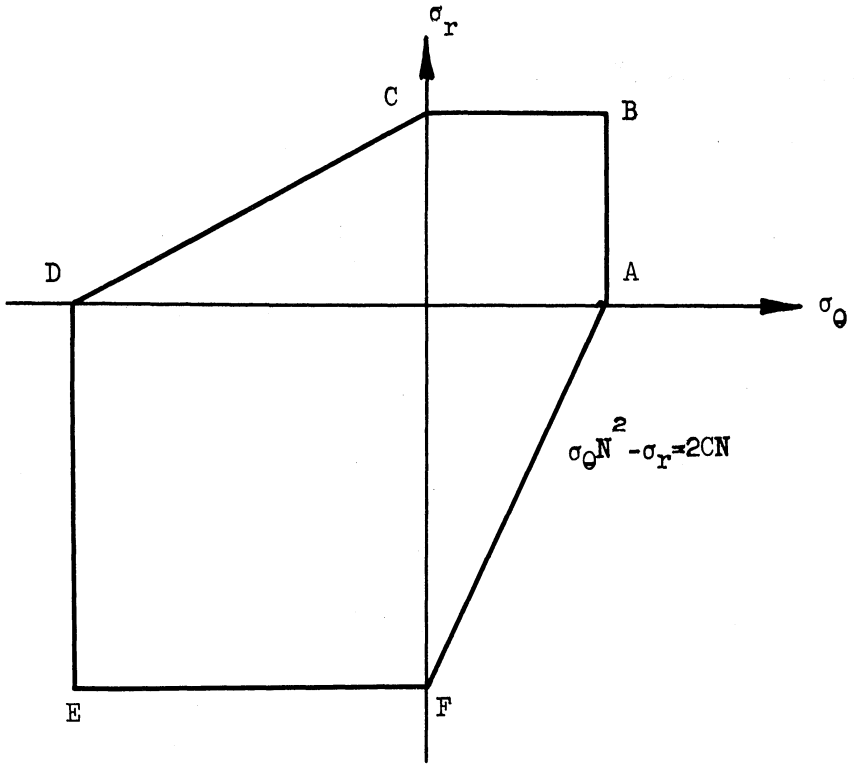

Fig. 4-1. Plane stress section of Coulomb yield criterion.

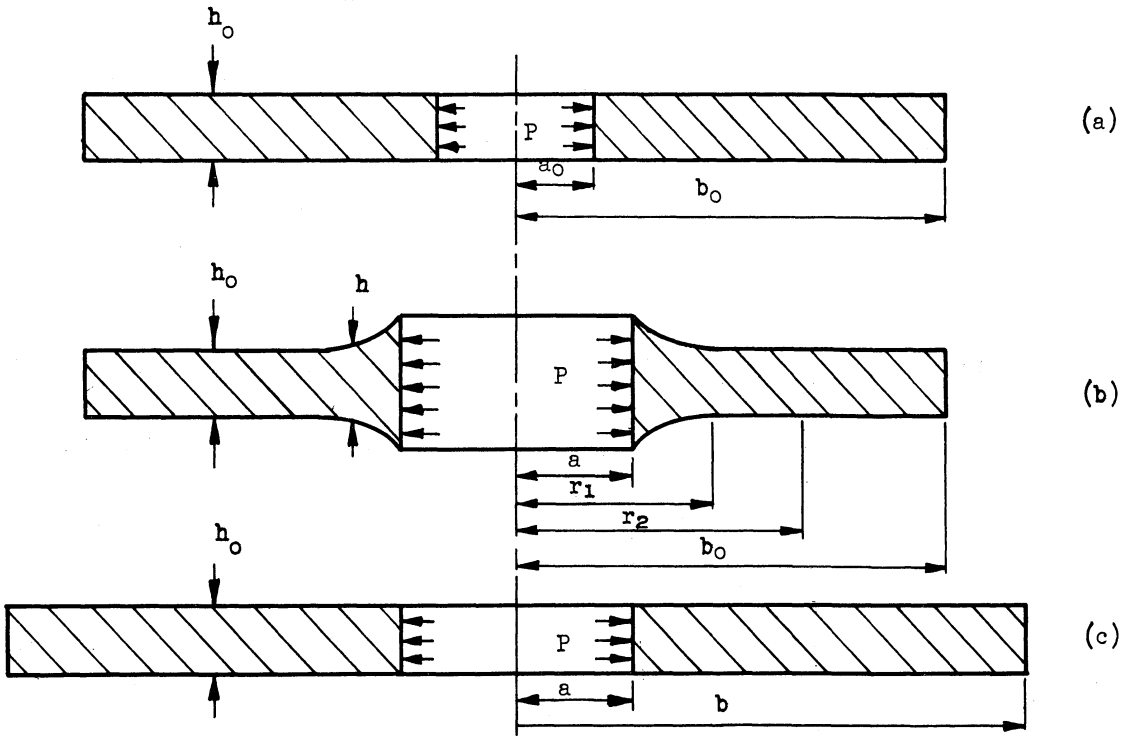

Fig. 4-2. Annular plate. a) Undeformed plate, b) Type I deformation of the plate, c) Type II deformation of the plate.

Because the problem is axially symmetric, $\tau_{r\theta} = 0$ and the one equation of equilibrium for a plate of variable thickness is

$$\frac{\partial}{\partial r}(h\sigma_r) + \frac{h}{r}(\sigma_r - \sigma_\theta) = 0 \tag{4.1}$$

where h is a function of r.

The velocity-strain rate equations are

$$\dot{\epsilon}_r = \frac{\partial \dot{u}}{\partial r}, \quad \dot{\epsilon}_\theta = \frac{\dot{u}}{r}, \quad \text{and } \dot{\epsilon}_z = \frac{1}{h}\frac{Dh}{Dt} \tag{4.2}$$

where $\dot{u}$ is the radial velocity; $\dot{\epsilon}_z$ is the strain rate in the z direction averaged through the thickness; and $\frac{D}{Dt}$ denotes the rate of change following an element, i.e. the material derivative given by

$$\frac{D}{Dt} = \frac{\partial}{\partial t} + \dot{u}\frac{\partial}{\partial r}. \tag{4.3}$$

The two regimes of Fig. 4-1 that will be needed for this problem are AF and F and the equations associated with these are:

For regime AF

$$\sigma_z = 0 \text{ and } \sigma_\theta N^2 - \sigma_r = 2CN \tag{4.4}$$

where C is the cohensive strenth, ϕ is the angle of friction, and N^2 is related to ϕ by the equation $N = \tan(\frac{\pi}{4} + \frac{\phi}{2})$. It should be noted that $\phi = 0$ implies that $N^2 = 1$ and the yield criterion coincides with the Tresca yield criterion. The strain rates satisfy the equations

$$\dot{\epsilon}_z = 0 \text{ and } \dot{\epsilon}_\theta + \dot{\epsilon}_r N^2 = 0. \tag{4.5}$$

For regime F

$$\sigma_z = 0, \ \sigma_\theta = 0, \ \sigma_r = -2CN, \text{ and} \tag{4.6}$$

$$\dot{\epsilon}_\theta + \dot{\epsilon}_z + N^2\dot{\epsilon}_r = 0. \tag{4.7}$$

Equation (4.5) is due to R.T. Shield [26]. R.M. Haythornthwaite [27] has shown that the second form, Equation (4.7), is necessary at certain corners.

With the aid of Equations (4.2) and (4.3), Equations (4.4) and (4.5) can be put in terms of the displacement and the thickness. For regime AF, Equations (4.5) become

$$\frac{Dh}{Dt} = 0, \quad N^2 \frac{\partial \dot{u}}{\partial r} + \frac{\dot{u}}{r} = 0, \tag{4.8}$$

and for regime F Equation (4.7) becomes

$$N^2 \frac{\partial \dot{u}}{\partial r} + \frac{\dot{u}}{h}\frac{\partial h}{\partial r} + \frac{1}{h}\frac{\partial h}{\partial t} + \frac{\dot{u}}{r} = 0. \tag{4.9}$$

The above equations together with the appropriate boundary conditions will allow one to determine the stresses, strain rates, velocities, changes in thickness, and displacements in the proposed problem.

B. SOLUTIONS

The solution of this problem will depend on the size of the plate, i.e. the magnitude of b_0/a_0. If the plate is large (b_0/a_0 large), then the entire plate will not deform plastically, and there will be a region near the outer radius of the plate which will remain rigid. If the plate is small enough, the entire plate will deform plastically. These two solutions will be identified as type 1 for the plate with both a deforming and a rigid region, and type 2 for the fully plastic

region. The critical value of b_0/a_0 which separates the type 1 solution from the type 2 will be found and it will be shown to depend only upon the material property N^2.

1. Type 1 Solution

For the type 1 solution there is some radial distance, say r_2 in Fig. 4-2b, at which the plastic region of the plate ends and the rigid region begins. At this interface, the stresses must satisfy the yield criterion and equilibrium but for $r_2 \leq r \leq b_0$ stresses must be found that are everywhere at or below yield and satisfy equilibrium. Such stresses may be found from the elastic solution (e.g., See I.S. Sokolnikoff [36]).

$$\sigma_z = 0, \ \sigma_r = A - \frac{B}{r^2}, \text{ and } \sigma_\theta = A + \frac{B}{r^2} \qquad (4.10)$$

where A and B are constants for any given state of stress but vary as the straining proceeds.

At the radius $r = r_2$, the stresses given by Equations (4.10) reach the yield surface at side AF, Fig. 4-1, and at $r = b_0$, $\sigma_z = 0$. These conditions together with Equations (4.10) give

$$\sigma_r = \frac{2CNr_2^2b_0^2}{r_2^2(N^2-1)+b_0^2(N^2+1)}\left[\frac{1}{b_0^2}-\frac{1}{r_3^2}\right] \text{ and } \sigma_\theta = \frac{2CNr_2^2b_0^2}{r_2^2(N^2-1)+b_0^2(N^2+1)}\left[\frac{1}{b_0^2}+\frac{1}{r_2^2}\right]. \qquad (4.11)$$

These stresses are below yield and satisfy equilibrium for all $r_2 \leq r \leq b_0$.

For $r \leq r_2$, one seeks a solution such that the stress point remains on regime AF. On this regime the second of Equations (4.8) together with the boundary condition that $\dot{u} = 0$ at $r = r_2$, leads to $\dot{u} = 0$. This can be used together with $\dot{\epsilon}_z = 0$ to give

$$\frac{\partial h}{\partial t} + \dot{u} \frac{\partial h}{\partial r} = 0. \tag{4.12}$$

Thus h does not change with time and therefore there is no thickening of the plate as long as the stress point remains on regime AF.

Because $\dot{u} = 0$ and $h = h_0$ for $r \leq r_2$, there is no motion in this region even though the stresses are on regime AF. Therefore, to complete the solution, it is necessary to find another region on the range $r \leq r_2$ for which motion can take place. Before this can be done the extent of the non-deforming plastic region must be found and for this the stresses are needed.

To find the stresses for a stress point on regime AF, Equations (4.1) and (4.4) with h = constant give

$$\frac{\partial \sigma_r}{\partial r} + \frac{\sigma}{r} \left(\frac{N^2-1}{N^2}\right) = \frac{2CN}{rN^2}. \tag{4.13}$$

The boundary condition associated with Equation (4.13) is found from Equation (4.11) to be

$$\sigma_r = \frac{2CN(r_2^2-b_0^2)}{N^2(r_2^2+b_0^2)+(b_0^2-r_2^2)} \quad \text{at } r = r_2. \tag{4.14}$$

Combining Equations (4.13) and (4.14) gives

$$\sigma_r = \frac{2CN}{N^2-1}\left[1 - \frac{2b_o^2N^2}{(r_2^2+b_o^2)N^2+(b_o^2-r_2^2)}\left(\frac{r_2}{r}\right)^{\frac{N^2-1}{N^2}}\right]. \quad (4.15)$$

Now from Equations (4.15) and (4.4) σ_θ is found to be

$$\sigma_\theta = \frac{2CN}{N^2-1}\left[1 - \frac{2b_o^2}{(r_2^2+b_o^2)N^2+(b_o^2-r_2^2)}\left(\frac{r_2}{r}\right)^{\frac{N^2-1}{N^2}}\right]. \quad (4.16)$$

It should be noted that by taking $N^2 = 1 + \epsilon$ in Equations (4.15) and (4.16) the solution for the Tresca yield criterion can be approximated to any desired degree of accuracy by taking ϵ to be sufficiently small. However, because of the obvious singularity in these equations, the solution for the Tresca yield criterion, which is expressed in terms of $\ln(r/r_2)$, cannot be obtained by replacing N^2 by 1. This same situation recurs throughout the entire analysis.

The above solutions apply only when the stress point is on regime AF. By taking $\sigma_\theta = 0$ in Equation (4.16) and solving for r, the value of r, say r_1 of Fig. 4-2b, at which the stress point reaches regime F of Fig. 4-1, is found to be

$$r_1 = \frac{r_2}{\left[\frac{N^2+1}{2}\right]^{N^2/(N^2-1)}}. \quad (4.17)$$

On regime F, $\sigma_\theta = 0$ and $\sigma_r = -2CN$, and Equation (4.1) reduces to

$$\frac{\partial h}{\partial r} + \frac{h}{r} = 0. \quad (4.18)$$

Thus

$$h = \frac{h_o r_1}{r} \quad (4.19)$$

after integration and use of the boundary condition $h = h_0$ at $r = r_1$.

Equation (4.9) can be used to find the velocity $\dot{u}$. There is a differentiation with respect to time in Equation (4.9) but since there is no viscosity, all of the rates can be taken with respect to any variable which increases monotonically as the applied load increases. It is convenient to use r_1 as the measure of time. Then, in view of Equation (4.18), Equation (4.9) becomes

$$\frac{\partial}{\partial r}(\dot{u}N^2) + \frac{1}{r_1} = 0 \tag{4.20}$$

and so

$$\dot{u} = \frac{1}{N^2} - \frac{r}{r_1 N^2} \tag{4.21}$$

after use of the boundary condition $\dot{u} = 0$ at $r = r_1$. The final radius (a of Fig. 4-2b) of the hole can be found from Equation (4.7). This can be rewritten as

$$\dot{\epsilon}_\theta + \dot{\epsilon}_z + \dot{\epsilon}_r = (1-N^2)\dot{\epsilon}_r. \tag{4.22}$$

The right side of Equation (4.22) is known because $\dot{\epsilon}_r$ is known. The left side of Equation (4.22) is the time rate of change of the change of the volume per unit volume. Thus

$$\dot{\epsilon}_\theta + \dot{\epsilon}_z + \dot{\epsilon}_r = (1-N^2)\dot{\epsilon}_r = \frac{\dot{\Delta V}}{V} \tag{4.23}$$

where V is the current volume of the deformed material, i.e., all of the material inside the radius r_1 and $\dot{\Delta V}$ is the time rate of change of the volume inside this radius.

Now if a_0 is the initial radius of the hole and a its present radius, then the change in volume is given by

$$\Delta V = \int_a^{r_1} 2\pi h r dr - \pi h_o [r_1^2 - a_o^2]. \tag{4.24}$$

The rate of volume change per unit volume is then

$$\dot{\Delta V} = \frac{d}{dr_1} \left[\int_a^{r_1} 2\pi h r dr - \pi h_o [r_1^2 - a_o^2] \right]. \tag{4.25}$$

An alternative expression for $\dot{\Delta V}$ can be found by substituting the values of the strain rates found from Equation (4.21) into Equation (4.23):

$$\dot{\Delta V} = \frac{N^2-1}{N^2 r_1} \int_a^{r_1} 2\pi h r dr. \tag{4.26}$$

Hence

$$\frac{d}{dr_1} \left[\int_a^{r_1} 2hr dr - h_o [r_1^2 - a_o^2] \right] = \frac{N^2-1}{N^2 r_1} \int_a^{r_1} 2hr dr. \tag{4.27}$$

The thickness h is given by Equation (4.19), and the radius a is a function of r_1 which is to be determined. Equation (4.27) is equivalent to

$$\frac{da}{dr_1} = \frac{1}{N^2} \left[1 - \frac{a}{r_1} \right] \tag{4.28}$$

and with the boundary condition $a = a_o$ when $r_1 = a_o$, the solution is

$$a = \frac{r}{N^2+1} \left[1 + N^2 \left(\frac{a_o}{r_1} \right)^{\frac{N^2+1}{N^2}} \right]. \tag{4.29}$$

The radial displacement u can be found from the definition of the velocity

$$\dot{u} = \frac{Du}{Dt} = \frac{\partial u}{\partial r_1} + \dot{u} \frac{\partial u}{\partial r}. \tag{4.30}$$

Eliminating $\dot{u}$ between Equations (4.21) and (4.30) gives

$$N^2 \frac{\partial u}{\partial r_1} + \left(1 - \frac{r}{r_1}\right) \frac{\partial u}{\partial r} = 1 - \frac{r}{r_1} . \qquad (4.31)$$

Assuming a solution of the form $u = r_1 F(\nu)$, where $\nu = r/r_1$ leads to

$$\frac{u}{r_1} = (1+N^2) \left\{ - \frac{r}{r_1} + \left[\frac{-1+(N^2+1)\frac{r}{r_1}}{N^2} \right]^{\frac{N^2}{N^2+1}} \right\} \qquad (4.32)$$

where use has been made of the boundary condition $u = 0$ at $r = r_1$.

The type 1 solution is now complete and it is possible to find the range of the ratio b_0/a_0 for which the solution is valid. Whenever $r_2 \geq b_0$ the solution will not be valid because there will be no rigid region. Setting $r_2 = b_0$ in Equation (4.17) gives

$$r_1 = b_0 (N^2)^{\frac{N^2}{N^2-1}} \qquad (4.33)$$

To relate r_1 to a, Equation (4.29) is used. Recalling that $r_1 = a_0$ when $a = a_0$ (the boundary conditions associated with Equation (4.28)), one obtains

$$\frac{b_0}{a_0} = (N^2)^{\frac{N^2}{N^2-1}} . \qquad (4.34)$$

Thus when $(b_0/a_0) > (N^2)^{\frac{N^2}{N^2-1}}$, the type 1 solution is valid, the limit load being $P = 2CN$. When $(b_0/a_0) \leq (N^2)^{\frac{N^2}{N^2-1}}$ the entire plate will be plastic and will be associated with regime AF of Fig. 4-1.

It should be noted that the type 1 solution is an exact solution of the plane stress problem. However, it cannot be an exact solution to the three-dimensional problem, for finite displacements, because the thickness of the plate changes. This change of thickness has been accounted for in the equation of radial equilibrium but, at finite dis-

placements, the stress boundary conditions have not been satisfied.

2. Type 2 Solution

For the type 2 solution, the entire plate is on regime AF and the stresses can be found from Equations (4.1) and (4.4) when h is known. It is possible to find h from the first of Equations (4.8) by first finding the velocity $\dot{u}$ from the second of Equations (4.8). As in the type 1 solution, the time derivatives can be taken with respect to any variable which is monotonically increasing with the load and in this case the radius a is used. The second of Equations (4.8) gives

$$u = C_2\left(\frac{a}{r}\right)^{\frac{1}{N_2}} \tag{4.35}$$

where the constant C_2 is non-zero because the entire plate is plastic and therefore $\dot{u}$ cannot be identically zero. Also, C cannot be determined without arbitrarily specifying the velocity of one point. Therefore, by taking $\dot{u} = 1$ at $r = a$ the velocity for any radius is given in terms of the velocity of the inside radius. For this choice, C_2 is unity. Combining Equation (4.35) with the first of Equations (4.8), with $v = a/r$ and assuming $h = h(v)$, leads to

$$\frac{dh}{dv}\left[\frac{1-(v)^{\frac{1+N^2}{N2}}}{r}\right] = 0. \tag{4.36}$$

Since $1 - (v)^{\frac{1+N^2}{N2}}$ cannot be identically zero, dh/dv must vanish, and one concludes that

$$h = h_0. \tag{4.37}$$

Now combining Equations (4.1) and (4.4) with $h = h_0$ and using the

boundary condition $\sigma_r = 0$ at $r = b$ one obtains

$$\sigma_r = \frac{2CN}{N^2-1}\left[1 - \left(\frac{b}{r}\right)^{\frac{N^2-1}{N^2}}\right] \tag{4.38}$$

and

$$\sigma_\theta = \frac{2CN}{N^2(N^2-1)}\left[N^2 - \left(\frac{b}{r}\right)^{\frac{N^2-1}{N^2}}\right]. \tag{4.39}$$

Equation (4.38) is used to determined the limit load by taking $\sigma_r = -P$ at $r = a_o$, $b = b_o$, the result being

$$\frac{P}{2CN} = \frac{1}{N^2-1}\left[-1 + \left(\frac{b_o}{a_o}\right)^{\frac{N^2-1}{N^2}}\right]. \tag{4.40}$$

Equation (4.40) gives the limit load for $1 \leq (b_o/a_o) \leq [N^2]^{\frac{N^2}{N^2-1}}$ and from the type 1 solution $P/2CN = 1$ for $(b_o/a_o) \geq [N^2]^{\frac{N^2}{N^2-1}}$. Therefore, the limit load is known for any size of plate and the results are shown graphically in Fig. 4-3 for $N^2 = 2$, $N^2 = 3$, and $N^2 = 4$.

To complete the type 2 solution the displacement u must be found. This displacement can be found from Equation (4.35) which can be written as

$$\frac{dr}{da} = \dot{u} = \left(\frac{a}{r}\right)^{\frac{1}{N^2}}. \tag{4.41}$$

The boundary conditions associated with Equation (4.41) are

$$r = r \text{ at } a = a$$

and (4.42)

$$r = r_o \text{ at } a = a_o.$$

The initial coordinate of a point is given by r_o and its final coordinate by r. The initial coordinate of a point can be related to its

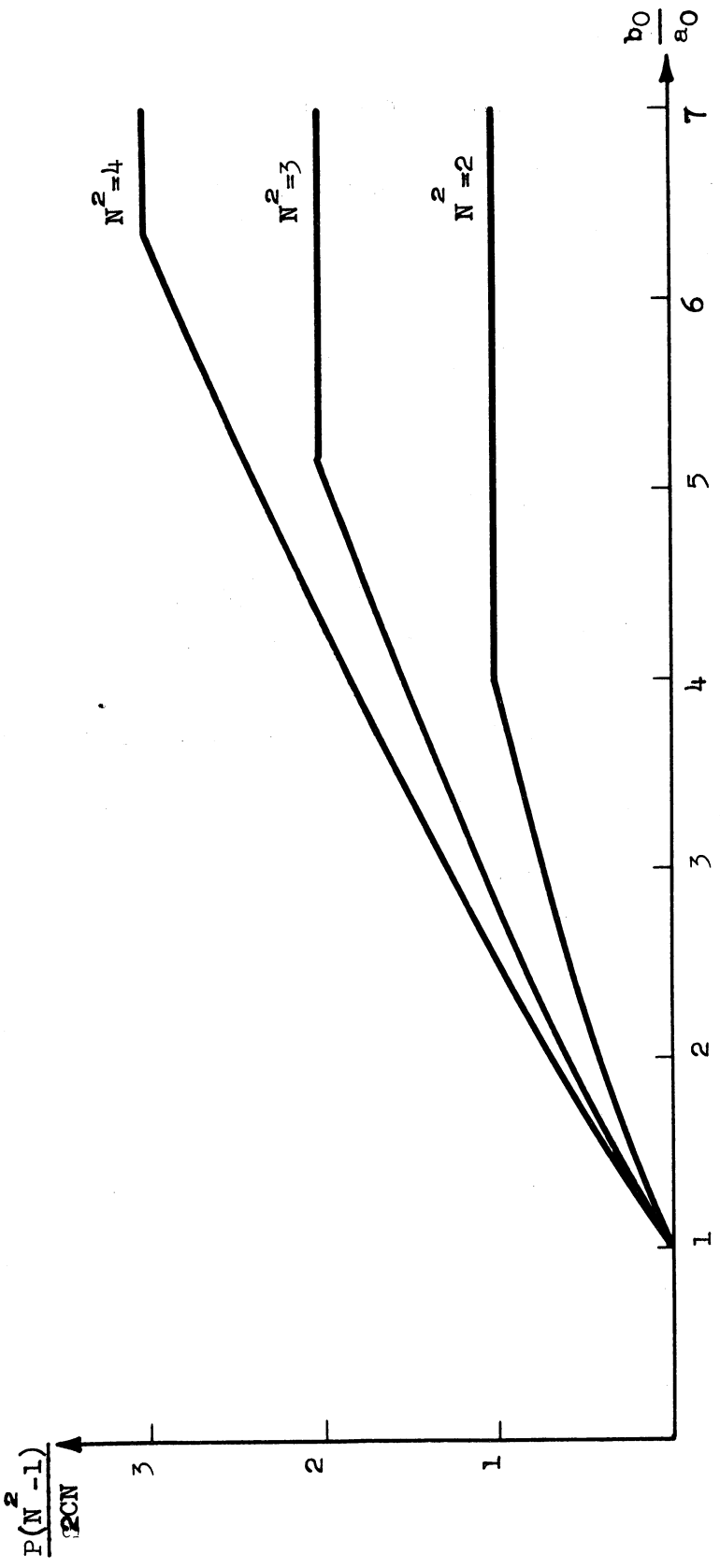

Fig. 4-3. Limit load of annular plate as a function of plate size.

final coordinate through the displacement, expressed in terms of the final coordinate, by

$$r_0 = r - u(r,a). \tag{4.43}$$

By separating Equation (4.41) and using the boundary conditions in Equation (4.42), one obtains

$$\int_{r-u}^{r} r^{\frac{1}{N^2}} dr = \int_{a_0}^{a} a^{\frac{1}{N^2}} da. \tag{4.44}$$

From Equation (4.44), u is found to be

$$u = r - \left(r^{\frac{1-N^2}{N^2}} - a^{\frac{1-N^2}{N^2}} + a_0^{\frac{1-N^2}{N^2}} \right)^{\frac{N^2}{1-N^2}}. \tag{4.45}$$

The type 2 solution is not only an exact solution for the plane stress problem, but also for the three-dimensional problem because there is no thickening of the plate.

CHAPTER V

CONCLUSIONS

The techniques used in this work were essentially the same as those used for an incompressable material in which the yield is unaffected by mean stress. However, the details of obtaining solutions were more complicated because the Coulomb yield criterion and its associated flow rule were used. In the cylindrical shell problem the procedure for determining the yield surface in terms of the stress resultants was the same as that which has been used for the Tresca criterian, but the types of deformation which were possible were more complicated because of the dilatation. Also, the procedure for determining the extent of the deformable region in the annular plate problem was the same as for the Tresca and Mises criteria, but the details were again more complicated because of the dilatation.

The determination of the shape and extent of the deformable region in the shell and the annular plate was made easier because the shape of the deformable region in both cases was known a priori. In each case, the extent of the deformable region was a function of only one variable. Thus it is far from clear that situations possessing less natural symmetry can be solved completely by a parallel technique.

In the problems considered here, the exact yield surface could be used because it proved possible to single out appropriate facets of this surface by a systematic procedure. In the beam and shell

problems, the correct regimes of the yield surface were determined by first considering the possible modes of deformation, whereas in the annular plate problem, the correct regimes of the yield surface were found by first considering the stresses.

The specific results concerning the problems solved here can be summarized as follows:

A. LIMIT ANALYSIS OF BEAMS AND PLATES IN CYLINDRICAL BENDING

The yield surface for a beam of rectangular cross-section has been found in terms of the moment and the axial force. This yield surface was used to determine the limit load for two beams with different end conditions. The first beam considered is loaded by a concentrated force at the center and is restrained from rotation, but not extension, at both ends. Secondly, a beam is considered in which the ends are restrained from both rotation and extensional motion. The limit load has been obtained for both cases and the limit load for the beam which is allowed no extensional motion is higher. Also in this case there is an axial force in the beam at the limit load.

B. LIMIT ANALYSIS OF A CYLINDRICAL SHELL

The yield surface for a cylindrical shell has been found in terms of the longitudinal and circumferential normal stress resultants and the longitudinal moment. This yield surface shows the effect of the sensitivity of the yield criterion to mean stress.

This yield surface was used to obtain the limit load for a cylindrical shell loaded by a ring of pressure. Two different cases were considered. One in which the ring of pressure is applied from the inside and the other with a ring of pressure applied from the outside. The limit loads for both types of loading were found to be an increasing function of N^2. However, the limit load for the externally applied load is greater than that for the internally applied load for all values of $N^2 > 1$. This difference is a result of the dependence of the Coulomb yield criterion on mean stress.

C. PLASTIC ANALYSIS OF AN ANNULAR PLATE

The limit load for all ratios b_0/a_0 of the outside radius to the inside radius has been found. The limit load is a function of the material property N^2 which is related to the angle of friction of the material. A critical ratio has been found which separates two different modes of failure. For b_0/a_0 less than the critical value, the entire plate deforms by expansion with no thickening and the limit load is a function of b_0/a_0. However, for b_0/a_0 greater than the critical value, only a portion of the plate near the inside radius deforms and the remainder of the plate is rigid at the limit load. For the second case, the plate does thicken as the load increases above the limit load. However, for this case, the limit load is independent of b_0/a_0, i.e., the plate is effectively infinite.

In addition to the limit load the stress distribution, velocities, displacements, thickening, and the extent of the deforming region has been found for finite displacements, being limited only by the assumption of plane stress.

REFERENCES

1. Hill, R. 1950. The Mathematical Theory of Plasticity, Oxford University Press, New York.

2. Kirkpatrick, W.M. 1957. The condition of failure for sands, Proc. 4th Intern. Conf. Soil Mech. and Found. Eng., 1: 172-181.

3. Haythornthwaite, R.M. 1960. Mechanics of the triaxial test for soils, Proc. ASCE, SM5, 86: 35-62.

4. Wu, T.H., A.K. Loh, and L.E.Malvern. 1963. Study of failure envelope of soils, Proc. ASCE, SM1, 89: 145-181.

5. Murphy, G. 1957. Properties of Engineering Materials, International Textbook Co., Scranton, Pa.

6. Akroyd, T.N.W. 1962. Concrete Properties and Manufacture, Pergamon Press Inc., New York, pp. 6-20.

7. Technical Data on Plastics, 1952. Manufacturing Chemists' Assoc. Inc., Washington.

8. Butkovich, T.R. Dec. 1954. Ultimate strength of ice, Snow, Ice and Permafrost Research Establishment, Corps of Engineers, U.S. Army, Research Paper 11: 1-11.

9. Butkovich, T.R. Oct. 1956. Strength studies of sea ice, ibid., 20: 1-15.

10. Butkovich, T.R. Oct. 1956. Strength studies of high-density snow, ibid., 18: 1-19.

11. Prager, W. 1954. An Introduction to Plasticity, Addison-Wesley, Reading, Mass.

12. Onat, E.T. and W. Prager. 1953. The influence of axial forces on the collapse loads of frames, Proc. 1st Midw. Conf. Solid Mech: 40-42.

13. Haythornthwaite, R.M. 1957. Beams with full end fixity, Engineering, 183: 110-112.

14. Haythornthwaite, R.M. 1961. Mode change during the plastic collapse of beams and plates, Develop. in Mech. 1: 203-205.

REFERENCES (Continued)

15. Onat, E.T. and R.M. Haythornthwaite. 1956. The load-carrying capacity of circular plates at large deflection, J. Appl. Mech. 23: 49-55.

16. Onat, E.T. and W. Prager. 1953. Limit analysis of arches, J. Mech. Phys. Solids, 1: 77-89.

17. Drucker, D.C. 1953. Limit analysis of cylindrical shells under axially-symmetric loading, Proc. 1st Midw. Conf. Solid Mech: 158-163.

18. Eason, G. and R.T. Shield. 1955. The influence of free ends on the load carrying capacities of cylindrical shells, J. Mech. Phys. Solids, 4: 17-27.

19. Sawczuk, A. and P.G. Hodge, Jr. 1960. Comparison of yield conditions for circular cylindrical shells, J. Franklin Inst., 269: 362-374.

20. Hodge, P.G., Jr. 1954. Rigid plastic analysis of symmetrically loaded cylindrical shells, J. Appl. Mech., 21: 336-342.

21. Onat, E.T. 1955. Plastic collapse of cylindrical shells under axially symmetrical loading, Q. Appl. Math. 13: 63-72.

22. Onat, E.T. and W. Prager. 1954. Limit analysis of shells of revolution, Proc. Roy. Netherland Acad. Sci. B 57: 534-548.

23. Hodge, P.G., Jr. 1960. Yield conditions for rotationally symmetric shells under axisymmetric loading. J. Appl. Mech., 27: 323-331.

24. Hodge, P.G., Jr. 1961. The Mises condition for rotationally symmetric shells, Q. Appl. Math., 18: 305-311.

25. Drucker, D.C. and R.T. Shield. 1959. Limit analysis of a symmetrically loaded thin shell of revolution, J. Appl. Mech., 26: 61-68.

26. Shield, R.T. 1955. On Coulomb's law of failure in soils, J. Mech. Phys. Solids, 4: 10-16.

27. Haythornthwaite, R.M. 1960. Mechanics of the triaxial test for soils, Proc. ASCE, SM5, 86: 35-62.

REFERENCES (Concluded)

28. Taylor, G.I. 1948. The formation and enlargement of a circular hole in a thin plastic sheet, Q. J. Mech. & Appl. Math., 1: 103-124.

29. Hill, R. 1949. Plastic distortion of non-uniform sheets, Phil. Mag., 40: 971-983.

30. Prager, W. 1953. On the use of singular yield conditions and associated flow rules, J. Appl. Mech., 20: 317-320.

31. Hodge, P.G., Jr. and R. Sankaranarayanan. 1958. On finite expansion of a hole in a thin infinite plate, Q. Appl. Math., 16: 73-80.

32. Sokolovsky, V.V. 1961. Expansion of a circular hole in a rigid/plastic plate, Appl. Math. and Mech. [Transl. of PMM] 25: 809-815.

33. Nordgren, R.P. and P.M. Naghdi. 1963. Finite twisting and expansion of a hole in a rigid/plastic plate, ASME Trans. Series E 30: 605-612.

34. Alexander, J.M. and H. Ford. 1954. On the expanding a hole from zero radius in a thin infinite plate, Proc. Roy. Soc. A, 226: 543-561.

35. Nordgren, R.P. and P.M. Naghdi. 1963. Loading and unloading solutions for an elastic/plastic annular plate in the state of plane stress under confined pressure and couple, Intern. J. Engin. Sci., 1: 33-70.

36. Sokolinkoff, I.S. 1956. Mathematical Theory of Elasticity, 2nd ed., McGraw-Hill, New York, p. 300.